Applied Materials Today 50 (2026) 103214

Contents lists available at ScienceDirect

Applied Materials Today

journal homepage: www.elsevier.com/locate/apmt

Advances in foam extrusion of micro- and nanocellular polymers: Strategies for controlling cell size and open-cell content

Marcos Merillas [a,b], Miguel Ángel Rodríguez-Pérez [a,b], Judith Martín-de León [a,b], Victoria Bernardo [a,b,*]

[a] CellMat Laboratory, Campus Miguel Delibes, Faculty of Science, Condensed Matter Physics Department, University of Valladolid, Paseo de Belen 7, 47011 Valladolid, Spain

[b] BioecoUVA Research Institute, University of Valladolid, Spain

ARTICLE INFO

Keywords:
Polymer foam
Extrusion
Review
Nanocellular polymer
Microcellular foam

ABSTRACT

Extrusion foaming is a key industrial technology for the production of lightweight polymer foams widely used in many markets. Recently, growing interest has focused on micro- and nanocellular polymer foams due to their outstanding combination of properties. To date, the fabrication of such materials has been restricted to laboratory-scale processes. Among foaming technologies, foam extrusion stands out as the most promising route for scaling up the production of micro- and nanocellular polymers. However, achieving fine cellular structures while maintaining low density and process stability remains a major challenge due to the intrinsic characteristics of the extrusion process. Therefore, extending extrusion foaming towards micro- and nanoscale structures requires a deep understanding of the underlying physical mechanisms to design production process able to achieve such structures. This review provides a comprehensive overview of the strategies reported in the literature to control cellular architecture in extrusion foaming, particularly the cell size and cell interconnectivity. First, the fundamental principles of extrusion foaming are summarized. Then, approaches for cell size reduction are discussed, including blowing agent selection, processing conditions, and the use of nucleating agents, ranging from conventional mineral fillers to nanoscale and self-assembling additives. Special attention is given to mechanisms governing cell nucleation, growth, coalescence, and stabilization, highlighting the trade-offs between cell refinement and foam density. In addition, strategies aimed at promoting controlled open-cell structures are reviewed, given their growing relevance for some advanced applications. The effects of melt strength modification and the introduction of heterogeneities are examined. Finally, a critical outlook on current limitations and the underlying causes of process and material constraints is discussed. Open challenges and future research directions are also presented. Overall, this review provides a unified framework linking formulation, processing, and cellular structure in extrusion foaming. By identifying the key factors governing cell size reduction and open-cell formation, it aims to guide future design of formulations and processes for the manufacturing of high-performance polymer foams with controlled micro- and nanocellular open-cell structures.

Abbreviations: ER, Expansion ratio; R, Anisotropy ratio; PS, Polystyrene; XPS, Extruded polystyrene; EPS, Expanded polystyrene; PU, Polyurethane; PE, Polyethylene; LDPE, Low density polyethylene; PP, Polypropylene; HMS-PP, High melt strength polypropylene; PLA, Polylactid acid; PET, Polyethylene terephthalate; PTFE, Polytetrafluoroethylene; POE, Polyolefin elastomer; BTA, Benzene trisamide; SEBS, Styrene ethylene butylene styrene; PESU, Polyethersulfone; PEG, Poly ethylene(glycol); EPDM, Ethylene propylene diene monomer; PMMA, Polymethyl methacrylate; TPS, Thermoplastic starch; VIP, Vacuum insulation panel; PBA, Physical blowing agent; CFC, Chlorofluorocarbons; HCFC, Hydrochlorofluorocarbons; HFC, Hydrofluorocarbons; HFO, Hydrofluoroolefin; ODP, Ozone depletion potential; GWP, Global warming potential; CNT, Carbon nanotube; CNF, Carbon nanofiber; EG, Expanded graphite; AC, Activated carbon.

* Corresponding author at: CellMat Laboratory, Campus Miguel Delibes, Faculty of Science, Condensed Matter Physics Department, University of Valladolid, Paseo de Belen 7, 47011 Valladolid, Spain.

E-mail address: victoria.bernardo@uva.es (V. Bernardo).

https://doi.org/10.1016/j.apmt.2026.103214
Received 4 February 2026; Received in revised form 25 March 2026; Accepted 3 April 2026
Available online 7 April 2026

1. Introduction

1.1. Polymer foams: concepts and fabrication routes

Polymer foams are two-phase materials that consist of a cellular-structured solid polymeric matrix, which contains a gaseous phase inside the cells. These materials have been developed since the early 20th century and hold great value in many industries, such as energy, construction, automotive, packaging, or even clothing, thanks to their high-performance properties in a great number of areas, including thermal and acoustic insulation, impact damping or lightweight, among others [1,2].

The properties of cellular polymers, like their mechanical and thermal behavior, are governed not only by the polymer matrix that constitutes the solid phase, but also by their structural characteristics. The main parameters used to characterize cellular polymers are depicted in Fig. 1.a. The density of the foam (ρ) is probably the most important one, as it gives information about the solid to gas ratio of the foam. Density influences every single property of the resultant foam. Besides the density, it is common to use dimensionless parameters derived from it to provide information about the ratio of the solid and gas phases. For instance, relative density (ρ_r) can be used, which is the ratio between the density of the foam and that of the solid precursor, that is, the solid fraction of the material. The inverse parameter, volume expansion ratio, often referred to as ER can also be used to quantify the volumetric expansion with respect to the solid material. The cellular structure can be characterized by the cell size (ϕ), which is the average diameter of the cells in the foam, and the anisotropy ratio (R), which is the ratio between two diameters in perpendicular directions of the cell. The cell size has a strong influence on the thermal conductivity, while the anisotropy ratio deeply impacts the mechanical performance. Related to cell size, there is another useful parameter often used to quantify the homogeneity of the structure: the normalized standard deviation coefficient SD/ϕ. As the structure of foams has a distribution of cell sizes and homogeneity, the standard deviation of all the measured cell diameters can be calculated (SD) and normalized by the average cell size to calculate this parameter. The homogeneity of the structure can depend on different aspects like processing conditions, materials or production methods. Cell density, N_V, and nucleation density, N_0, are two key parameters that give a general insight about the foam. The first one is the volumetric density of cells in the final foam, while the latter is the density of nuclei formed prior to cell growth and foam expansion. Finally, the open-cell content (OC) indicates how interconnected the inner structure is, being an important parameter for several properties such as acoustic, mechanical, or permeation to liquids/gases, among others.

These and many other characteristics of cellular materials are profoundly influenced by the fabrication route (i.e., foaming method) employed. The gas used, and the way it is introduced inside the polymer, as well as the polymer choice itself, significantly influence the final properties of the foam. Foaming methods can be chemical or physical, depending on how the foam is produced: chemical processes can involve the thermal decomposition of a chemical blowing agent like azodicarbonamide, or reactive foaming, used for example in polyurethane foaming. In physical foaming methods, a physical blowing agent (like CO_2 or N_2) is directly introduced into the polymer. Among these physical fabrication routes, four stand out and are widely used both in industry and research: batch foaming, bead foaming, injection molding, and extrusion foaming. These processes are sketched in Fig. 1.b.

In batch foaming processes, the precursor, usually in its solid state, is introduced inside a high-pressure vessel and later saturated with gas pressure. When the gas is released and pressure suddenly drops, the gas molecules form clusters known as nuclei that later evolve into cells [3]. Batch foaming can be either a one-step or a two-step process, depending on the temperature of the polymer at the moment of the pressure release. If it is high enough, the polymer will have enough mobility to allow expansion during pressure release, so nucleation and expansion will occur immediately after pressure release (one-step) [4]. In contrast, if the temperature is low at the moment of pressure release, the precursor will require extra heating for foaming (two-steps) [5,6]. Batch-foaming is commonly used in the lab-scale thanks to the wide range of pressure and temperatures that can be used, as well as deep control of all process stages. Nevertheless, the size of the pressure vessel limits the dimensions and geometry of the produced foams. Bead foaming is essentially a batch foaming process where many small polymer beads are foamed in suspension inside a stirred, water-filled pressure vessel [7], usually to be molded or thermoformed afterwards into a more complex-shaped part, so a secondary process is needed to achieve the final product. In contrast, injection processes differ from these two, as it involves processing a polymer/gas melt rather than a solid precursor, and share some similarities with extrusion-based techniques. In foam injection molding, the polymer is heated above its glass transition or melting temperature and extruded through a screw where gas is also injected [8]. The gas/-polymer melt is then injected into a mold, forced to expand with a determined shape and volume. The final product usually comes with a thick skin due to the fast cooling of the polymer in the mold surface, and the final expansion is limited due to gas solubility and process temperature constraints [9]. All these three processes (batch foaming, bead foaming, injection molding) have one thing in common: they are batch/discontinuous processes. In the first two, an autoclave or pressure vessel must be opened and closed each time the precursors are placed inside or taken out, and saturation processes normally involve long times (usually hours). Foam injection molding is faster, but the mold

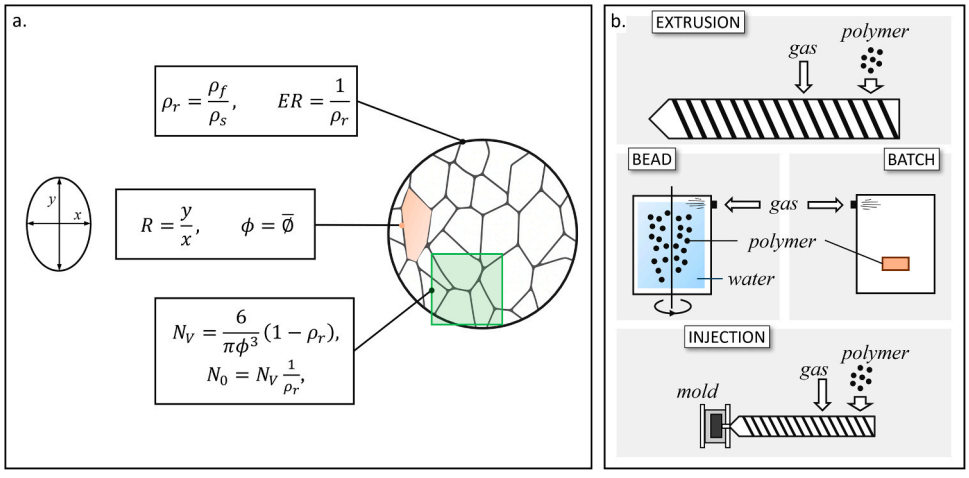

Fig. 1. (a.) Main parameters for cellular polymers characterization. (b.) Main physical foaming methods.

must be removed and emptied each time a sample is made. The only foaming process to produce large quantities of continuous polymer foam is extrusion foaming.

Extrusion foaming involves saturating a molten polymer with a blowing agent during the extrusion process, followed by a rapid pressure drop that induces nucleation and cell growth [2]. It possesses critical differences with the previously mentioned processes. Compared to autoclave-based methods, in which the material remains in a semi-solid state during foaming, extrusion foaming operates on a fully molten polymer. In this sense, it is similar to injection molding, but both processes require significantly different conditions. Foam injection molding is a discontinuous process in which the polymer/gas mixture is injected into a closed mold, leading to rapid cooling, high pressure gradients, and limited expansion. In contrast, extrusion foaming is a continuous process where the saturated melt flows through a die under more stable thermal and pressure conditions, allowing to achieve very low densities and generally improved structural homogeneity.

Apart from being continuous, extrusion foaming is scalable, and thus it is applied nowadays in the industry for numerous different ends. For instance, extruded polystyrene (XPS) production has already surpassed one million metric tons per year and is only expected to keep growing in the near future [10]. While traditional extrusion foams are widely used in packaging and insulation, new interest is focused on pushing the boundaries of this technology toward new regimes, such as micro- and nanometric cell sizes, where our current knowledge often falls short.

1.2. Micro- and nanocellular polymers: structure and properties

During most of the 20th century, cellular materials with relatively large cell sizes (above 50 μm) were commonly produced. This was primarily due to limitations in manufacturing technologies, which made it difficult to precisely control cell morphology. Still today, conventional foams such as polyurethane foams (PU), expanded polystyrene (EPS), and extruded polystyrene (XPS) typically exhibit cell diameters ranging from 50 to 500 μm. However, significant advancements in foaming techniques—either through the development of new methods or the refinement of existing ones—led to a major breakthrough in the later decades of the century with the production of microcellular polymers, characterized by cell sizes below 10 micrometers [2,11]. At the beginning of the new century, the cell size was reduced even more, below the micron: nanocellular polymers were born. The reduction of the cell size in polymeric foams can induce dramatic changes in the performance of the materials [12–15]. For instance, reducing the size of the XPS cells to the microcellular range (< 10 μm) and ultimately to the nanocellular range (< 1 μm) can greatly enhance thermal and mechanical performance [16,17]. Microcellular materials can achieve a balance between low density and mechanical properties, increasing stiffness. Nanocellular materials go even further, potentially achieving ultra-low thermal conduction through the gas phase [18,19], high surface-to-volume ratios, and even optical transparency in some cases [20] (when the pores are smaller than 50 nm), while other mechanical properties also keep improving [21].

These features of micro- and nanocellular polymers offer a new range of possibilities in growing sectors such as refrigeration, high-efficiency buildings, or biomedical devices [12]. However, the process of achieving such small cell sizes is complex and still far from a real application in the industry. First, nucleation density must be in the range of 10^{14}–10^{16} nuclei/cm^3 to reach the nanoscale cell size regime, 7 orders of magnitude above conventional foams [22]. As seen in the equations of Fig. 1.a, the cube of cell size and the density of the foam are inversely proportional to N_0, which explains why a very high number of nuclei is required to obtain very small cell diameters, keeping the density low. For this reason, the enhancement of nucleation or cell density will lead to cell size reduction. While other methods could produce nanoporous films [23,24], as mentioned before, batch foaming is the only process allowing to generate nanocellular polymer foams with large dimensions, particularly high thickness, and usually requires the use of extreme conditions (high pressures or low temperatures) to promote high and efficient nucleation [12,22]. Pore sizes ranging from 10 μm to decades of nm can be achieved with this technology, and the limit in pore size is greatly related to the polymer nature and its limitations rather than the process itself. For instance, pressures above 20–30 MPa are usually reported in batch foaming, sometimes in combination with temperatures even below 0 °C and in many cases near room temperature [20,25]. These features make it rather easy to achieve small cell sizes with this foaming route (for example, 14 nm with 550 kg/m^3 has been achieved with PMMA [20] and 440 nm with 300 kg/m^3 with PS [26]). Such demanding conditions allow to maximize gas solubility, but cannot be reproduced in a continuous process. Moreover, as briefly commented before, this is a batch process with discontinued production and limitations in the size and shape of the samples due to the geometry constraints of the pressure vessel, which strongly limit scalability. Thus, new production processes closer to the industry are needed to transfer these materials from the lab-scale to real applications.

One of the best alternatives, considering all the excellent features mentioned above, would be foam extrusion. However, in extrusion foaming, the own nature of the process makes the task of reducing the cell size much more challenging. The high temperatures employed and the architecture of the machines limit the process conditions, thus limiting cell nucleation in comparison with batch foaming. This is why an in-depth understanding of the underlying mechanisms taking place inside the extruder is needed to be able to fine-tune the cellular structure to the micro- and/or nanometric range.

Furthermore, beyond reducing the cell size to the micro- or nanometric range, achieving controlled open-cell structures represents an additional and particularly demanding challenge in extrusion foaming. In this process, the mechanisms governing cell wall rupture are strongly coupled to the processing conditions. Nevertheless, being able to tune the interconnectivity of micro- and nanocellular foams significantly expands their range of applications. Open-cell micro- and nanocellular foams can be used in applications in which conventional foams do not apply, such as microfiltration and drug-release devices [27,28]. Moreover, they are also attractive as core materials for Vacuum Insulation Panels (VIP), where an open-cell inner structure with small pores is required to evacuate the gas, allowing a reduction of the thermal conductivity of the material up to 75%. While commercial fumed-silica VIPs can give thermal conductivities below 5 mW/(m·K), they are expensive and heavy (200 kg/m^3). Foam-based VIPs, for example, PS-based VIPs, can reach thermal conductivities around 6–8 mW/m·K with much higher cost-efficiency and densities lower than 100 kg/m^3 [29].

1.3. Scope and objective of the review

The present work, outlined in Fig. 2, aims to provide a comprehensive roadmap for industry and scientific researchers interested in the design and scale-up of extruded micro- and nanocellular polymers. Specifically, it focuses on the techniques that control cell size and open-cell content, two key parameters that directly impact functionality in high-performance applications. The review takes into account the critical interplay between all the factors involved in the process: polymer formulation —matrix and its characteristics, blowing agent selection, addition of nucleating agents of different natures— and the processing conditions, like the pressure drop or the temperature.

2. Fundamentals of foam extrusion

2.1. Extruded polymer foams: examples and market applications

Extrusion foaming has been a key polymer processing technology for nearly a century. The first major milestone came in 1931 with the patent for XPS [30–32], marking the beginning of its widespread industrial use, particularly in thermal insulation and packaging. Since this

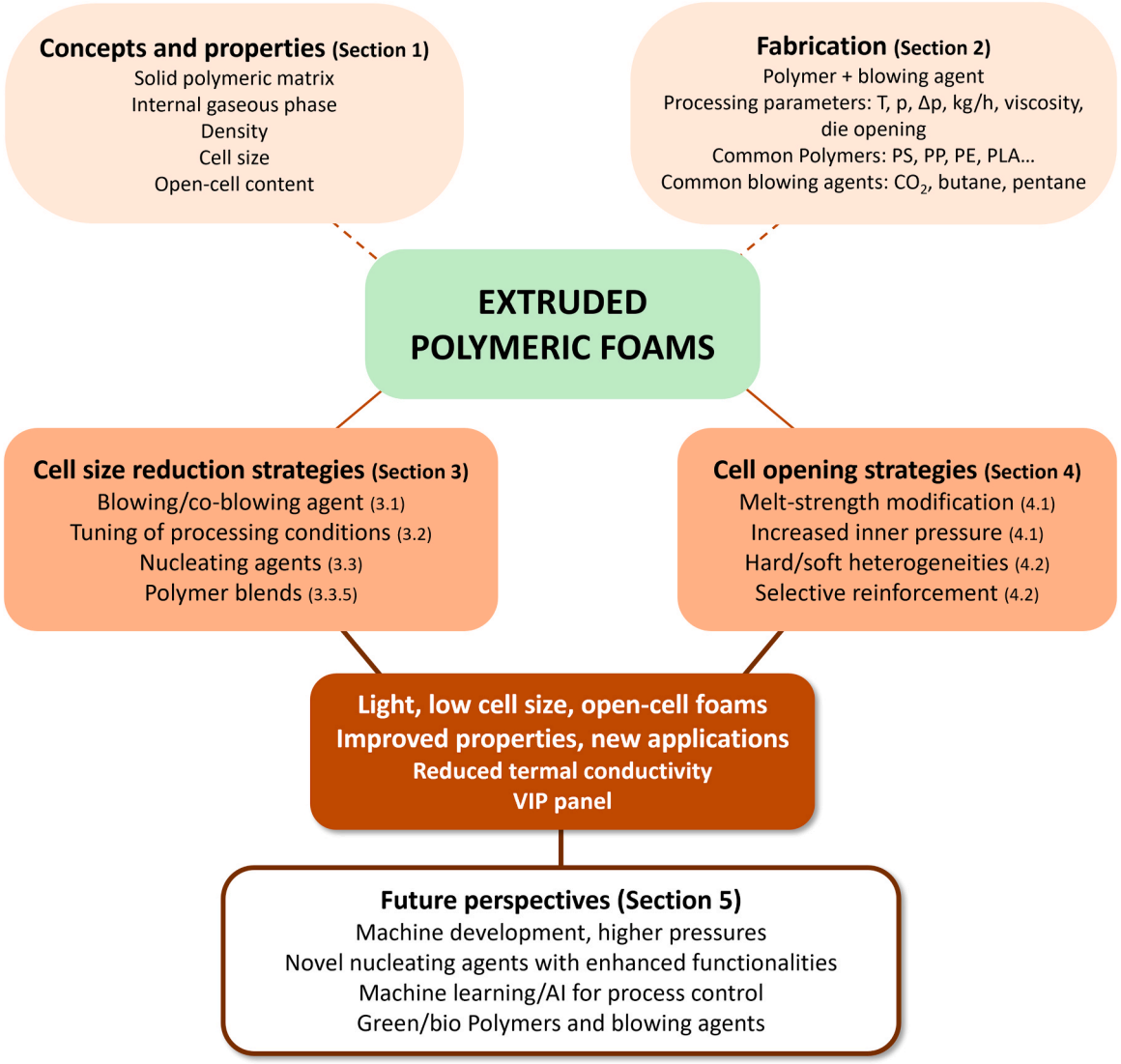

Fig. 2. General map depicting an overview of the work. Sections where each topic is discussed are included between brackets.

breakthrough, many advances were made throughout the whole 20th century, both in the development and improvement of the hardware and the implementation of other polymers, such as polyethylene (PE) [33] or polypropylene (PP) [34]. In recent years, due to the increase in environmental concerns, the use of biopolymers like poly(lactic acid) (PLA) has risen significantly [35].

These diverse choices of polymer matrices in combination with functional additives offer a wide range of properties that enable manufacturers to tailor foam characteristics to specific end-use requirements. XPS remains one of the most prominent extruded foam materials, with a global market size exceeding USD 5.5 billion in 2024 [36]. Used mainly in the building sector, extruded polystyrene offers exceptional mechanical and thermal properties with very low density, and it is mainly used for technical solutions when high compressive strength or exposure to harsh conditions are needed. This way, it is often found in floors, roofs, or exterior walls. Polyethylene is the second most common material used worldwide in extrusion foaming [37], and its applications range from protective packaging and cushioning to high performance insulation in critical environments [38]. The third most common polymer is extruded polypropylene [39]. PP foams are widely utilized in construction, the automotive sector, and packaging. Their versatility stems from a balanced combination of low density, good chemical resistance, and excellent impact absorption, which makes them suitable for applications ranging from lightweight automotive components and vibration dampening to protective packaging and sports equipment. Additionally, extruded PP foams offer good thermal stability and recyclability [40,41], which aligns well with the increasing industry demand for sustainable materials. Regarding extruded PLA, packaging applications have already been explored and commercially applied. Thermoformed foam-extruded PLA sheets have been proven to work up to the standards of traditional polymers in food trays for certain applications [42,43].

2.2. *Equipment and routes*

Extrusion foaming processes generally involve a single-screw or twin-screw extruder integrated with a gas injection system. The extruder can be linear or tandem, where two extruders are combined for better control in the process parameters [44]. A schematic representation of the linear process is presented in Fig. 3.a. In both cases, the polymeric formulation is fed through a hopper, and the pellets melt inside the extruder barrel, through which the screw or screws (single-screw or twin-screw extruder) push the molten polymer. This part is where the temperatures of the process are higher in order to get a homogeneous melted polymer flow when the blowing agent is added. L/D is the screw length/screw diameter ratio, and it is an important parameter

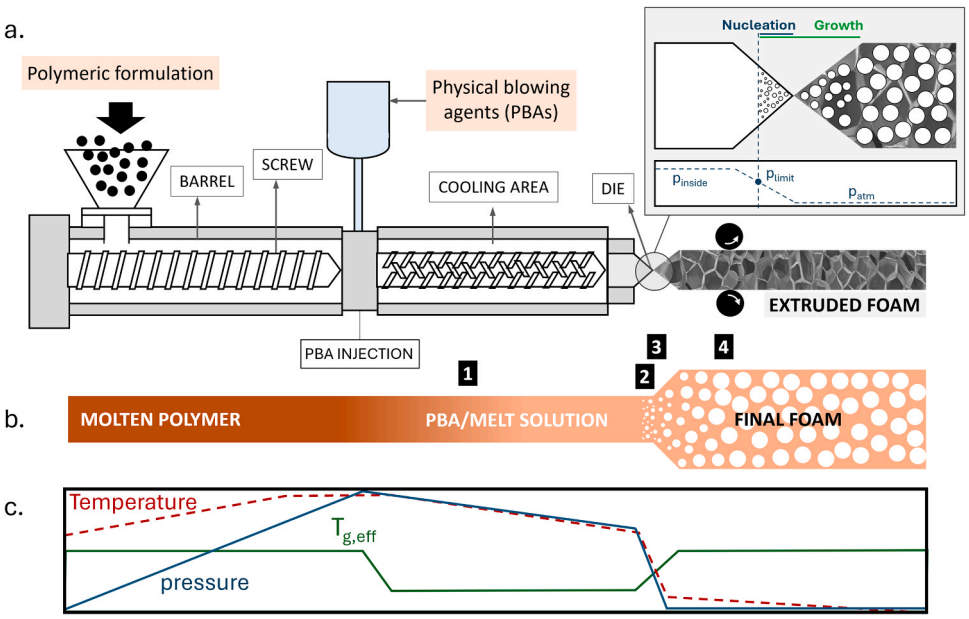

Fig. 3. a) Sketch depiction of the parts of the extruder, b) schematic representation of the extrusion foaming process, and c) the evolution main parameters involved in the process that influence the final foam.

commonly given in extrusion experiments. It can vary usually from 20 to 40, depending on the mixing and process control requirements, and the characteristics of the machine (single or twin screw, tandem extruder) [31]. The screw diameter can also vary from < 10 mm in lab-scale extruders [45] to 50–150 mm in common industrial lines [46] (even more in some cases). Normally, halfway through the extrusion path, the injection of the physical blowing agent (or blend of blowing agents) is performed. This blowing agent can be an inert gas (for instance, CO_2 or N_2), a hydrocarbon (pentane, butane, etc.), or other substances. The physical blowing agent is usually taken to supercritical conditions when injected into the extruder. The polymer/gas solution then passes through a cooling area, where the temperature of the melt is lowered in order to increase the viscosity to the right value before the expansion. In the case of amorphous polymers, blowing agents like CO_2 reduce the viscosity of the melt when they dissolve into the matrix (plasticization effect), so the temperature needs to be reduced considerably to have enough melt strength [47–49]. When the extruded polymer is semi-crystalline, the processing window will still be governed by the temperature of crystallization of the polymer, also affected by the presence of the gas, but not to the same extent [31,50]. In many cases, two or more blowing agents can be used, combining their effects and further enhancing the properties of the foam, as well as the processability of the melt. The cooling section can be a secondary extruder (tandem process) or a specific melt cooler whose architecture is designed to guarantee homogeneous temperature of the polymer. Finally, the polymer melt leaves the extruder through an aperture known as die, where the sudden pressure drop that takes place promotes nucleation, followed by cell growth and stabilization of the cellular structure. Correct growth and stabilization take place thanks to the adequate viscosity achieved during cooling and the instantaneous contact of the foam with ambient temperature, although some polymers might require extra cooling after leaving the die to assure stability. Additionally, the geometry of the die has a critical impact on the depressurization kinetics and thus on the final structure of the foam. Usually, the die has a initial conical shape that connects the barrel with the exit and a final cylindrical part (land length, usually very few mm), both of which can be used to shape the pressure gradient in the whole machine and, most importantly, the pressure drop and drop rate in the outlet, which is highly relevant for nucleation and growth of the foam [31,51].

2.3. Foaming mechanisms

The formation of cellular structures during extrusion is governed by a series of interconnected physical phenomena that can be broken down into four main stages: polymer/gas solution, nucleation, cell growth, and stabilization (Fig. 3.b tags 1–4). Understanding and controlling these stages is key to producing foams with desirable properties, particularly when targeting small cell sizes or specific properties, such as a determined open-cell content. These general stages can be better understood by considering a representative example.

In this context, a typical foaming process for XPS is going to be used to illustrate the underlying foaming mechanisms (Fig. 3). As stated in the previous paragraph, the foaming process begins with the dissolution of a blowing agent into the polymer melt (Fig. 3.b, tag 1). The solubility (the maximum uptake) and diffusivity (rate of sorption) of the gas in the polymer matrix, for a given polymer/blowing agent pair, are primarily governed by processing temperature and pressure, which are two key parameters controlling the foaming process [52–54]. A homogeneous polymer/gas solution is critical for uniform nucleation. Relatively high pressures (around 10 MPa or higher [53–55]) are needed to dissolve the blowing agent in the polymer matrix at the high temperatures needed to keep the polymer melted, especially when low densities are targeted (which require a very high amount of blowing agent). Also, shear during extrusion aids in the dispersion. Through gas pressure and melt temperature, the stability of the solution must be ensured so the polymer retains the gas without premature foaming or phase separation. Viscosity or melt strength of the polymer is key in this part of the process. As said in the previous section, when the blowing agent dissolves into the polymer, it normally induces a plasticization effect which, again, can be stronger or lighter depending on the polymer, the blowing agent, and the conditions in the extruder, due to the weakening of the molecular attractions in the matrix and the molecular movement induced. As a consequence, the glass transition temperature (T_g) of the saturated polymer is reduced (represented in the lower graph of Fig. 3.c, green line), and we can talk about an effective glass transition temperature ($T_{g,eff}$) [49,56]. Then, to gain viscosity, the temperature must be reduced in the cooling area.

In the proximity of the die, the saturated polymer/gas solution experiences a rapid pressure drop, inducing thermodynamic instability and initiating nucleation at the moment where the solubility limit is

surpassed (Fig. 3.b, tag 2). Gas molecules start to form clusters that form a nucleus that will eventually become a cell. The velocity at which the pressure drops (pressure drop rate) is a parameter of utmost importance in the nucleation process. Nucleation can be heterogeneous or homogeneous. Homogeneous nucleation takes place when there is only one phase (one homogeneous polymer matrix) or, if there is a second one, it is not promoting nucleation. In this case, gas molecules are the only agent influencing nuclei formation, and the process will follow the trends of the Classical Nucleation Theory (CNT) [57], that is, higher gas content will increase nucleation, and so will higher pressure drop rate, etc. Heterogeneous nucleation occurs when a second phase is added to the polymer with the intention that the nucleation energy barrier is lowered. When the second phase is constituted by inorganic nanoparticles, these obviously need to be smaller than the desired cells, well dispersed in the matrix, and in a sufficient number. When the pressure is released, the energy barrier is lower in the particle-polymer interphase, promoting the appearance of nuclei in those areas. In theory, the number of particles will determine the number of nuclei. This strategy is widely used to enhance nucleation and cell size reduction purposes, as it makes the foaming process much more efficient, though it also comes with some limitations. For example, it can imply mechanical weakening, normally due to aggregation of inorganic particles or just excess of filler in the walls affecting structural integrity [58]. Furthermore, the added particles can also have an impact on the process stability, as they can affect the viscosity of the melt and the shear rate in the machine, making it necessary to adapt the processing conditions with each particle concentration and even resulting in limited expansion if the concentration of particles is high [59–61].

Once the nuclei are formed, other dissolved gas molecules diffuse into them, promoting cell growth (Fig. 3.b, tag 3), which is mainly governed by the viscosity of the polymer, as it influences the gas diffusion rate and the ability of the polymer to expand at a given temperature [2]. In extrusion, temperature in the die is a key parameter that needs to be finely controlled as it affects both the melt and the gas characteristics and the way they interact with each other. Cells grow thanks to the temperature of the polymer coming out of the die being above its $T_{g,eff}$, and it stops when the cooling (both due to the expansion and ambient temperature) has taken the temperature of the foam below $T_{g,eff}$, which is constantly rising as the gas is diffusing outside the matrix (Fig. 3.c) [31].

After cell growth, the foam structure must be stabilized rapidly to preserve the desired cellular morphology (Fig. 3.b, tag 4). If the process is not properly controlled at this stage, degeneration mechanisms can appear. The two main cellular degeneration mechanisms in foam extrusion are coalescence and coarsening [62] (the third one, drainage, occurs mainly when the polymer phase has a very low viscosity, like in reactive processes). Coalescence can occur during cell growth, when the polymer has still high mobility: two or more cells merge due to the rupture of the cell wall between them. Also, cell opening can appear during this phase. If the walls are not strong enough to hold the growing pressure of the gas, they can break. If the breakage happens before the final expansion is reached, the density will be higher than expected. Coarsening refers to the growth of larger cells at the expense of smaller ones due to gas diffusion. It can happen during expansion or more normally during cooling, and it appears due to pressure differences between smaller (higher pressure) and larger (lower pressure) cells, which force the gas from small ones to bigger ones. In extrusion foaming, it is also critical that, at the conditions of the die, the gas does not escape too fast out of the polymer matrix, causing cell collapse or even shrinkage after production if the polymer is flexible [63]. To prevent these failures, foaming parameters must be finely tuned. The choice of a polymer with adequate viscosity and melt strength, and the temperature of the polymer/gas mix at the end of the machine, are key for the success of the process.

3. Strategies for reducing cell size

The reduction of the cell size in extruded foams remains one of the biggest challenges of this technology. The same factors that make extrusion foaming ideal for large-scale production of cellular materials also present significant challenges when foams with small cell diameters are wanted. The polymer is saturated at high temperatures that allow the gas dissolution to happen rapidly and in massive quantities of polymer continuously, but these same temperatures limit the solubility of gas in the polymer, as well as its viscosity (higher viscosity and melt strength can help control cell size). This is why the optimization of the processing conditions, along with the adequate blowing agent, must be the first issues to address to enhance nucleation and reduce the diameter of the cells. Apart from this, the most common strategy to enhance nucleation is the use of nucleating agents (mostly inorganic nano- or microparticles). These approaches are not mutually exclusive but rather produce better outcomes when implemented in conjunction. Considering other players, like the molecular weight of the precursor, polymer blends, and the blowing agents of choice for each case, may also help to optimize the outcoming foam.

3.1. Blowing and co-blowing agents

The blowing agent plays an important role in the properties of the foam. It controls the density and affects the cellular morphology [2]. The choice of physical blowing agents in polymer extrusion foaming has evolved under strong environmental regulation and performance constraints. Table 1 shows some of the most common PBAs in the past and recent years. Although CO_2 has been investigated as a blowing agent for decades, early foam production at an industrial level relied on chlorofluorocarbons (CFCs) from the 1930s to the 1980s, due to their low thermal conductivity and very low gas diffusion rates, which resulted in excellent thermal insulation performance [65]. These gases were banned due to their ozone depletion potential, as mandated by the Montreal Protocol in 1987 [66]. CFCs were subsequently replaced by hydrochlorofluorocarbons (HCFCs), which offered reduced ozone depletion potential but were still subject to phase-out due to their residual environmental impact. Later, hydrofluorocarbons (HFCs) were introduced; although they do not affect the ozone layer (ODP; see Table 1), they exhibit a relatively high global warming potential (GWP). As a result, HFCs were also progressively banned in Europe, and their use in extrusion foaming has been forbidden since 2014, driving the transition toward greener, low-GWP alternatives such as hydrocarbons (mainly butane and pentane), carbon dioxide (CO_2), nitrogen (N_2), and, in some cases, hydrofluoroolefins (HFOs).

In the current industrial picture, at least in the EU, hydrocarbons—n-butane and iso-pentane— and mixtures of CO_2 with EtOH are the most common strategies for foaming polystyrene and other commodity polymers by extrusion. When solutions of XPS with lower thermal conductivities are required, HFOs allow to reduce thermal conductivity of the XPS boards from 32 to 34 mW/m·K when foamed with CO_2 to 25–27 mW/m·K with HFO [67–69], thanks to the low thermal conductivity of the gas and its reduced diffusivity, that allows for the HFO to remain in the foam for longer times, while CO_2 escapes rather quickly.

The selection of the type and amount of blowing agent must be done considering the targeted structure and the polymer matrix. It is known that the solubility and diffusivity of the gas in the polymer, as well as their plasticization effect on the melt, will have a great impact on the resulting foam in terms of cell morphology, size, nucleation and, of course, foam density. According to Classical Nucleation Theory (CNT), one would expect cell size to decrease with an increase in the amount of blowing agent [70–72]. In practice, there is a gas solubility limit for each combination of gas and polymer (and obviously, pressure and temperature conditions) that needs to be considered. In an extrusion process, all the gas should be dissolved in the polymeric matrix to have a stable process that can be maintained and replicated.

Table 1
Some common physical blowing agents and their main physical and environmental characteristics (Mw ≡ Molecular weight, BP ≡ Boiling point, pc ≡ Critical pressure, Tc ≡ Critical temperature, FL ≡ Flamable limit in air, ODP ≡ Ozone depletion potential (CFC−11 =1), GWP ≡ Global warming potential (CO_2 = 1), λ ≡ Thermal conductivity, AL ≡ Atmospheric lifetime) [2,64].

PBA	Formula	Mw (g/mol)	p_c (MPa)	T_c (°C)	ODP	GWP	λ (25 °C) (mW/mK)	AL (years)	Polymer
Carbon dioxide	CO_2	44.0	7.4	31.0	0	1	16.4	120	PS, PP, PLA, PET, TPU*
Nitrogen	N_2	28	3.4	−146.9	0	-	25.8	-	PS*, PP*, PE*, PET*, TPU*
Water	H_2O	18.0	22.1	374.0	0	-	-	-	PS*,PP*,PE*
Ethanol	C_2H_5OH	46.1	6.1	241.0	0	-	14.4	-	PS
Propane	C_3H_8	44.1	4.3	96.8	0	11	17.9	Few days	PS, PE, PP
n-butane	C_4H_{10}	58.1	3.8	149.9	0	< 10	16.1	Few days	PS, PE, PP
iso-butane	C_4H_{10}	58.1	3.65	134.6	0	11	16.2	Few days	PS, PE, PP
n-pentane	C_5H_{12}	72.0	3.4	196.7	0	11	15	Few days	PS, PE
iso-pentane	C_5H_{12}	72.0	3.38	188	0	11	14.3	Few days	PS, PE
HCFC−22	CHF_2Cl	86.5	5.0	96.0	0.055	1900	10.7	11.8	PS, PE
HFC−152a	CHF_2CH_3	66.1	4.5	113.5	0	140	14.7	1.7	PS, PP, PE
HFC−134a	CH_2FCF_3	102.0	4.1	100.6	0	1600	13.8	14	PS, PE
HFC−245fa	$CHF_2CH_2CF_3$	134.1	3.6	157.5	0	950	13.3	7.4	PS
CFC−11	$CFCl_3$	137.4	4.4	198.0	1	4600	7.9	45	PS
CFC−12	CF_2Cl_2	120.9	4.1	112.0	1	10600	9.9	100	PS
HFO−1234ze(E)	$CFHCHCF_3$	114.0	3.6	109.4	0	< 1	13	19	PS, PP, PE

* Mostly lab-scale research.

Experimental results comparing different gases under similar extrusion conditions are scarce in the literature. Two works by Richard Gendron and Caroline Vachon [73,74] studied the performance of HFC−134a and CO_2 in polystyrene foaming. In the first of those two works, they measured the solubility of the gas in the polymer, plasticization or degassing pressure, amongst other characteristics of the blowing agents, and analyzed the foams produced by equivalent molar concentrations of the two gases. The work found that the solubility limit of HFC−134a in PS is higher than that of CO_2 and thus can induce a greater plasticizing effect in the matrix. Also, diffusivity is much slower, which has a direct effect on nucleation: the slow mobility of the HFC−134a when the foaming occurs prevents cell coalescence and favors nucleation control. Furthermore, this increase in nucleation slightly reduces the expansion. Foams produced with 3.1 wt% CO_2 have cell sizes in the range of 200 μm, with nucleation density of 10^6 nuclei/cm^3 and foam density of 46.9 kg/m^3, while the ones made with an equivalent molar concentration of HFC−134a (7.12 wt%) have cell diameters of 30 μm, nucleation increased by 3 orders of magnitude (10^9 nuclei/cm^3) and density of 54.7 kg/m^3. The subsequent work introduced, apart from the two single-gas foaming extrusion experiments, some samples extruded with mixtures of the two gases in different proportions. The work, based on the trends of cell sizes, which evolve gradually with the mixture and with a similar and narrow size distribution, suggests that gas molecules in the blends behave as a whole, homogeneous mixture, rather than forming independent clusters. Also, it is noticed that nucleation is greatly affected by adding a small amount of the secondary gas on both ends. The sorption kinetics of the two gases are shown in Fig. 4. These works suggest that the bigger the molecular weight of the gas, the lower the diffusivity, while solubility depends greatly on thermodynamic affinity rather than molecular weight alone. A high solubility would increase nucleation, as backed by the Sanchez-Lacombe equation of state and experimental works [54,75–78].

In CO_2 extrusion, it is common to add a secondary blowing agent to facilitate control over the processing conditions and help increase the stability of the production line, and it is usually EtOH, which helps achieve stable processing conditions. Another work by Gendron et al. explored different CO_2/EtOH proportions in polystyrene extrusion foaming and found that the addition of EtOH was beneficial for problems associated with solubility limits that promoted bad morphology and cell opening [79]. With CO_2 alone, a low-density foam (25 – 30 kg/m^3) with a homogeneous structure is difficult to obtain due to a relatively low solubility and high diffusivity of the gas in PS. When adding EtOH, this kind of foam can be produced at very stable conditions. The work shows how a good combination of both blowing agents can provide better expansion and homogeneity without compromising cell size.

Other studies are found where, instead of EtOH, water is used as the co-blowing agent in combination with CO_2. Water can be injected directly into the extrusion line or by water-carrying/hydrophilic particles added to the raw pellets. Several studies show that the addition of water to a CO_2-blown extrusion can be useful for lowering the density of the foams [80] and also to induce bi-modal structures [81,82]. A work by Raje et al. [83], achieving very small cell sizes (5 μm) with polyethersulfone/polyethylene(glycol) (PESU/PEG) blends, found that the

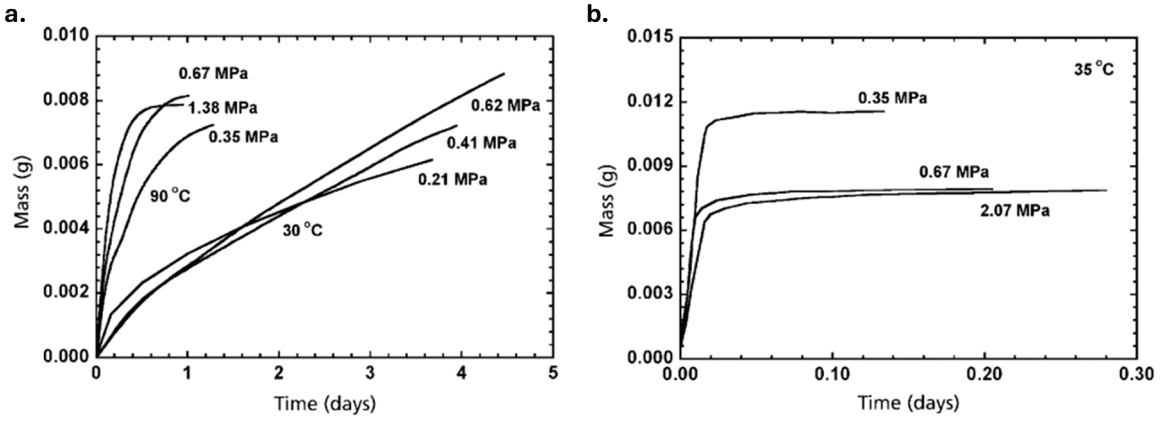

Fig. 4. Sorption kinetics of (a) HFC−134a and (b) CO_2 in polystyrene, from reference [73], reproduced with permission.

addition of H_2O to the CO_2 extrusion helped to achieve this cell size reduction and broaden the foaming temperature window (Fig. 5).

3.2. Processing conditions: pressure and temperature

Each combination of polymer, gas, and machine design has an optimum set of parameters regarding the objective of the process. Considering the scope of this section, there will be an optimum profile of pressure and temperature that will achieve the smallest cell diameters and highest nucleation. Of course, all these parameters affect each other greatly and do not change independently. For example, pressure will be directly affected, among other things, by the amount of blowing agent, the temperature profile of the machine, and the speed of the screw. Also, the pressure drop rate at the die will depend on its geometry, the temperature of the melt or inner pressure, amongst many other parameters. One can see the intertwining of these parameters in the predictions of the Classical Nucleation Theory for homogeneous nucleation [56]. Nucleation rate is predicted by Eq. 1, where f_0 is the frequency factor of gas molecules joining the nucleus, C_0 is the initial gas concentration, k_B is the Boltzmann constant and T is the temperature:

$$N = f_0 C_0 \quad \exp\left(-\frac{\Delta G_{hom}}{k_B T}\right) \tag{1}$$

The Gibbs free energy barrier (ΔG_{hom}) is the energy that the nucleus has to overcome to grow into a bubble, and it is given by Eq. 2:

$$\Delta G_{hom} = \frac{16\pi\gamma^3}{3\Delta p^2} \tag{2}$$

In this equation, γ is the surface tension between the gas and the polymer, and Δp is the difference between the gas and the solid pressure. According to Eqs. (1) and (2), one would expect a higher nucleation with a higher initial gas concentration, but also with a higher temperature and a higher pressure drop. Since temperature modifies viscosity, and thus the surface tension, the role of the different parameters is not always so clearly identified in real extrusion experiments.

Early works like the ones by Han and Oyanagi [84,85] start to explore these parameters with chemical extrusion foaming of PE and PS. Several key concepts are proven in these experiments, like how increasing temperature reduces the shear of the melt, and the density of the foams, or that nucleation is higher when decreasing the die aperture due to a higher pressure drop rate.

Later studies delve into these features, like the one by Park [86] analyzing the route to achieving microcellular structures with polystyrene by CO_2-blown extrusion foaming. In this work, Park uses 3 different nozzle lengths to analyze how the pressure drop in the die affects nucleation and its competition with cell growth. The longer the polymer/gas solution stays in the die, the more gradually the pressure drops (lower pressure drop rate), and thus nucleation happens for a longer period of time. This implies that many of the first-formed and growing nuclei will tend to receive gas molecules that could be forming one nucleus themselves. In these experiments, the authors manage to increase cell density from 10^8 to $7{\cdot}10^9$ cm^{-3} when changing from the longest to the shortest nozzle length. This variation in cell density (and subsequently nucleation) grows linearly with the pressure drops reported in the article. A second work addresses the need of controlling the processing temperature in order to increase melt strength and prevent coalescence during cell growth [87]. It proves that the expansion ratio depends on the melt and die temperature and can be maximized without affecting cell size if there is enough gas being injected into the machine. At high temperatures in the die, maximum expansion occurs very close to the die, and coalescence and contraction happen due to high diffusion and thin cell walls. When the temperatures decrease, diffusion is lowered, and the solid skin helps prevent gas escape.

X. Han et al. [88] made an experimental study combined with computational simulations that explored how the pressure drop, which is affected by CO_2 concentration and mass flow rate affects cell size and nucleation. It was proven that an increasing CO_2 concentration in the polystyrene melt shifted nucleation towards the inlet of the die. In the experiments with a fixed CO_2 concentration (of 2.5 wt%), they proved the direct relation between the pressure drop (modified by tuning the mass flow rate) and cell size and cell nucleation, as shown in Fig. 6, achieving a reduction from 13.8 to 7.5 μm when the pressure drop rate was increased from 3.4 to 12.7 10^8 $Pa{\cdot}s^{-1}$.

Peng [89] and colleagues designed an on-set visualization system shown in Fig. 7 with three camera inserts and three light sources on the opposite side of the die that allowed them to see how nucleation evolved along the die. At three different screw speeds that induced three different pressure profiles, they could prove that the lower the pressure, the sooner nucleation occurs, and obviously, the lower cell density and bigger cell diameter are obtained. For instance, they report a cell size of 76.3 μm at a screw speed of 9.2 rpm, which is lowered to 33.7 μm when the screw speed is tripled due to the increase of pressure, while cell density increases in one order of magnitude ($1 \cdot 10^6$–$1.5 \cdot 10^7$ cells per cm^3).

Few recent studies analyze processing conditions directly and in detail, as their modification is limited by the possibilities of the machine and has been widely studied in the past. Despite this fact, most of the literature shows some dependence on the processing parameters when studying other strategies to reduce the cell size (like the use of additives, developed in the next section). All in all, the pressure drop and drop rate in the die are probably the most important parameters when a reduction in cell size is wanted. Optimizing their values will guarantee fast and localized nucleation, so a homogeneous structure of small cells can be obtained. As shown in Fig. 6, increasing the pressure drop has a direct impact on the size of the cells in the final foam. Due to this being one of the most important parameters to reduce cell size, this reduction is ultimately limited by the pressure drop achievable for the machine. The stabilization of the foam is also crucial to maintain the desired structure.

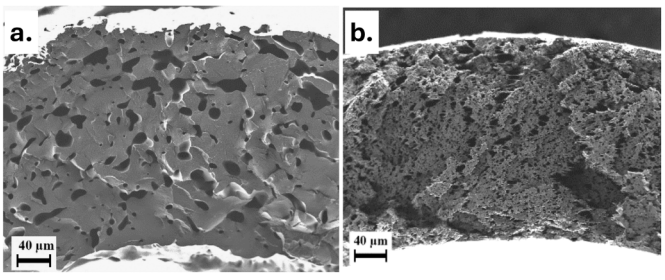

Fig. 5. PESU/PEG extruded foam (a) without and (b) with water aiding the process, from reference [83], reproduced with permission.

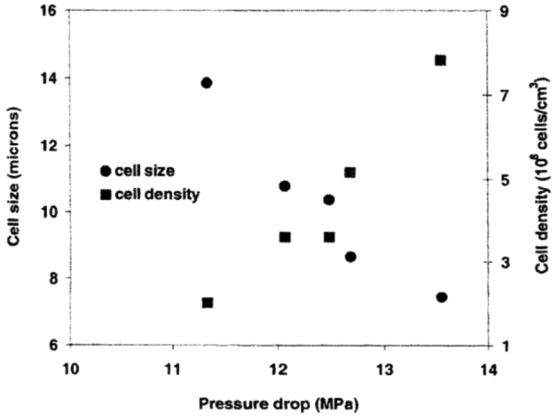

Fig. 6. Relation between cell size, cell density and pressure drop in a PS foam extrusion at 180°C with the same CO_2 content (2.5 w%), from reference [88], reproduced with permission.

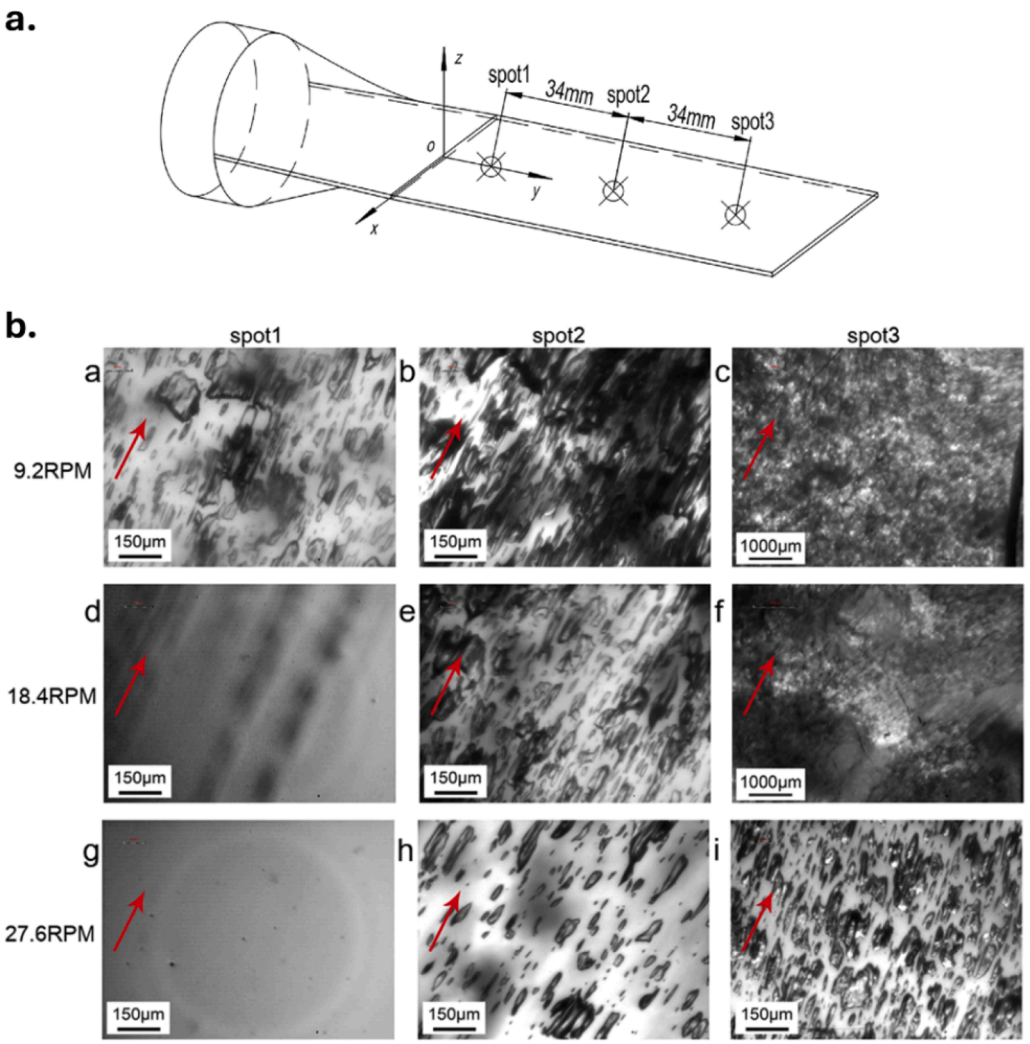

Fig. 7. (a) Sketch of the used set up for the visualization system. (b) Visualization images at the said three spots taken at various mass flow rates/27.6 rpm flow rate. Red arrow indicates the mass flow direction, from reference [89], reproduced with permission.

The temperature of the polymer at the exit has a direct impact on the melt strength and must be optimized to avoid further degeneration of the foam outside the machine, retaining the gas in the highest number of nuclei/cells possible, to achieve the smallest size. Only one work has been found that proves that, with machinery suitable to endure very high pressure, extrusion of nanocellular polymers is possible [90]. The work by Costeux showed the extrusion of a PMMA nanocellular polymer (see structure in Fig. 8), reaching a cell size of 300 nm thanks to an amount of dissolved CO_2 of 23%, with pressures of 45 MPa in the mixer and 36 MPa in the die. Under these conditions, hardly reproducible in a common extrusion foaming setup, they achieved extruded nanocellular foams, with a small area fraction (<10%) of micrometric cells and a large area occupied by the nanoscale pores. With this amount of gas dissolved in the PMMA matrix, plasticization is so strong that the temperature set in the die is lowered to just 38 °C (T_g of unsaturated PMMA is around 115 °C [91]). The density of these samples is 337 kg/m^3, and nucleation density is in the range of 10^{14} nuclei/cm^3.

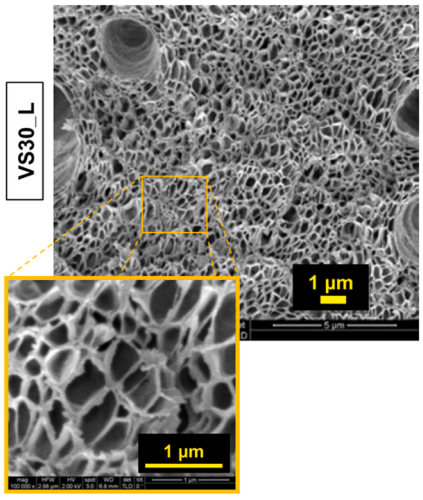

Fig. 8. Extruded nanocellular PMMA, from reference [90], reproduced with permission from the author.

3.3. Nucleating agents

A nucleating agent is a second phase that is added to the polymeric matrix to control or promote nucleation via heterogeneous nucleation. As shown in Eq. 3, according to the Classical Nucleation Theory, the energy barrier for heterogeneous nucleation, ΔG_{het}, is the same that for homogeneous nucleation (Eq. 2) multiplied by a factor S(ϑ), depending on the contact angle of the polymer-additive-gas interface. This factor is always lower or equal to one.

$$\Delta G_{het} = \Delta G_{\text{hom}}\, S(\theta) \quad (3)$$

That is, the introduction of nucleating agents reduces the energy barrier for nucleus formation, allows the generation of more nuclei, and thus achieving lower cell sizes.

Nucleating agents can be other polymers or copolymers, or can be particles like clays, silicas, or carbon nanotubes. The use of polymers or copolymers as nucleating agents relies on the nucleating efficiency of the organic phase to promote nucleation. For instance, in batch foaming, blends are often prepared via solvent casting or mechanical mixing, resulting in a dispersion of the second polymeric phase that remains stable during the foaming process, creating interphases to promote nucleation [60,92–94]. In extrusion foaming, due to the high temperatures employed in the process, the addition of another polymeric phase must be done carefully in terms of temperature control for an efficient promotion of heterogeneous nucleation. Apart from nucleation, the second polymer can also modify viscosity and affect cell growth and cell opening. Hence, most of the extrusion research found in the literature involves the use of nano- or micro particles when it comes to cell size reduction.

For efficient heterogeneous nucleation, particles must meet some requirements. Size should be small enough to have a very high number of particles per volume, even at very low concentrations. High aspect ratios and surface area have also been proven to be beneficial, as they maximize the interfacial particle-polymer surfaces [59]. That is, the geometry and nature of the particles are critical aspects controlling their effect in foaming. For this reason, particle size, surface area, aspect ratio, and also the geometry of the particles are listed in Table 2, which is a summary of the most common nucleating agents used in extrusion. Some of these particles are extensively used at an industrial scale, such as talc or some variants of carbon black particles, while others like nanosilica or carbon nanotubes, are mostly limited to research studies due to cost limitations.

Apart from their nucleating effect, in many cases, these particles can also enhance the mechanical properties of the foams, not only indirectly with the tuning of cell size, but through the reinforcement of the walls and struts of the cellular structure [95]. Furthermore, nucleating agents also tend to improve cell morphology homogeneity [113]. But despite numerous benefits, the reader will find that, in some cases, the materials produced with the use of nucleating agents are not as light as the pure ones. This is a common effect when heterogeneous nucleation is involved [94,114]. Yet, other cases are reported where the foaming window is shifted in a way that the highly-nucleated material also achieves a higher expansion. In the following paragraphs, the different nucleating agents listed in Table 2 and their effect in extrusion foaming are discussed. It must be noted that amorphous polymers behave differently from semi-crystalline ones when nucleating agents are added to the matrix. In semi-crystalline polymers, the effect of nucleating species is more complex, as they affect not only the cell nucleation, but also the crystallization dynamics of these polymers [115], while the effect on amorphous polymers is more straightforward. The most relevant results for each material are presented in the next sections and summarized in Table 3.

3.3.1. Talc

Talc is typically the first-choice nucleating agent in industrial polymer extrusion foaming processes thanks to its availability and low cost. It usually ensures consistent and even cell nucleation, which is crucial for process stability and product uniformity, making it the go-to option for balancing performance and cost-effectiveness with reliability in high-throughput, large-scale extrusion foaming. Many of the works referenced in this review use talc not as the subject of study, but as a reference rather than the pure polymer.

The effect of talc can be seen in the study by Okolieocha [95] in PS. With a content as low as 0.025 wt%, they managed to double cell density without affecting the density of the foam. With a higher content of 1 wt %, cell density increased by two orders of magnitude and cell size decreased from 400 to 100 μm, but in this case, the density of the foam increased by 20%.

Park [120] analyzed the effect of talc in the nucleation of extruded polypropylene, finding very different results depending on the blowing agent used (CO_2 or isopentane). While talc governs nucleation phenomena in the isopentane-blown experiments, with little dependence on the amount of gas, the effect of talc is only significant when the amount of CO_2 is small. These differences are attributed to the very different chemistry of the two gases. Later works by Naguib and Park [96,121,122] have deepened in the understanding of the nucleation mechanisms of talc in extruded PP foams with butane as a blowing agent. In these works, they analyze different talc contents (0.8, 1.6, and 2.4 wt%) in a wide range of die temperatures. While cell size is not discussed directly, cell density is clearly increased by one order of magnitude with the addition of 0.8 wt% talc compared to the neat polymer, achieving also a

Table 2
Nucleating agents/polymers and their main characteristics.

Nucleating agent	Chemistry / formulation	Particle size	Surface area (m^2g^{-1})	Shape	Aspect ratio	Ref.
Talc (mineral)	Hydrous Mg silicate	0.5–10 μm (thickness 1 μm)	2–20	Platelets	5–20	[95–99]
Nanoclays	Montmorillonite, organo-modified clays	100–1000 nm (thickness 1 nm)	200–800 (exfoliated)	Platelets	> 100	[99–105]
Nanosilica	SiO_2 nanoparticles	10–50 nm	200	Nearly spherical	1	[82,99]
Carbon nanotubes	Multi-walled CNTs (MWCNTs)	Ø 10–50 nm Length 1–20 μm	200–400	Tubes	100–1000	[95,106]
Graphene oxide (TRGO)	Single to few-layer graphene sheets	0.5–10 μm (thickness 1 – 10 nm)	400–2600	Platelets	> 100	[95]
Carbon nanofibers (CNFs)	Vapor-grown CNFs	Ø 100 nm Length 30–100 μm	Not specified	Fibers	50–200	[101, 107]
Activated carbon	Carbon particles	Ø 37 μm	Not specified	Quasi-spherical	1	[101]
Expanded graphite	Graphite flakes, thermally expanded	10–50 μm	50–300	Platelet-like	50–200	[108]
Micrographite (mGr)	Carbon particles	Not specified	Not specified	Irregular	Not specified	[106]
Calcium carbonate (nano/micro)	$CaCO_3$ (precipitated or nano-$CaCO_3$)	Nano: 20–100 nm Micro: 0.5–5 μm	15–40 (nano) 2–10 (micro)	Spherical	≈ 1	[109]
BTAs	Benzene-trisamides, urea-based self-assemblers	Ø 100–600 nm (length > 1 μm)	Not defined (forms in situ)	Nanofibrils	> 10	[110]
PTFE	Polymer that forms fibrils	Ø 300–600 nm (length > 400 μm)	Not defined (forms in situ)	Nanofibrils	> 500	[111, 112]

Table 3
Best results from some of the referenced works using nucleating agents. (Conc. ≡ concentration of nucleating agent; ρ_f ≡ foam density; φ ≡ cell size; φ↓ ≡ cell size reduction achieved by the addition of the nuc. Agent, regarding cell size when foaming the pure polymer or the reference polymer; Nv ≡ cell density of the foam).

Polymer	Nuc. Agent	Conc. (wt%)	ρ_f (kg/m^3)	ϕ (μm)	ϕ ↓ (%)	N_v (cm^{-3})	Ref
PS	talc	1	48	100	75	1.08×10^6	[95]
PP	talc	2.4	27	51*	77	1.14×10^7	[96]
PE	talc	0.35	48	245*	42	1.10×10^5	[97]
PLA	talc	0.5	890	33	79	8.61×10^6	[98]
PLA	talc	0.5	22	70*	65	5.32×10^6	[99]
PS	CNF	5	691	4.1	53	1.50×10^9	[107]
PS	CNF	0.5	31	116	55	1.18×10^6	[101]
PS	GR	0.5	29	75	71	4.40×10^6	
PS	AC	1.5	740*	75	71	1.35×10^6	
PS	MWCNT	1	52	65	84	2.87×10^6	[95]
PS	TRGO	1	60	25	94	5.58×10^7	
PS	MWCNT	1	110	100	43	2.44×10^6	[106]
PS	mGr	1	100	100	43	1.08×10^6	
PET	MWCNT	0.5	568	50	43	8.32×10^6	[116]
PS	nanoclay Cloisite 20 A	5	700	4.9	81	1.50×10^9	[117]
PS	nanoclay Cloisite 30B	1	41	60	92	8.50×10^6	[81]
PP	nanoclay Cloisite 20 A	5	48	22*	90	1.74×10^8	[103]
PP	Silica	0.5	Not spec	Not spec	Not spec	7.70×10^6	[118]
PE	Modified organoclay DK1	0.6	25	700	30	8.06×10^8	[104]
PLA	nanoclay Cloisite 30B	5	Not spec	0.2	Not spec	Not spec	[105]
PLA	Silica (Aerosil A 200)	1	35	35*	83	4.33×10^7	[99]
PLA	nanoclay Clositie 30B	1	34	11*	95	1.39×10^9	[99]
PS	nano-$CaCO_3$	5	440*	28.7	91	4.62×10^7	[109]
PS	BTA	0.2	78	18	97	1.50×10^8	[119]
PP	PTFE	0.3	32	48	79	3.39×10^8	[111]
PP	PTFE	4	100	110	63	1.60×10^7	[112]

higher expansion ratio when talc is added. The effect is not so pronounced at higher loads, but increasing the talc content keeps increasing cell density in a very wide range of processing temperatures, as Fig. 9 shows. These works also analyzed the effect that the talc addition has on the crystallization kinetics of PP, finding that talc particles decreased the mobility of the polymer molecules and led to early crystallization, resulting in a higher crystallization temperature and higher crystallinity. There was also a clear effect on the operating temperature for optimal expansion ratio: Samples containing talc reached their peak expansion at cooler temperatures. The authors state that, at high temperatures, a quicker gas loss due to higher cell density is responsible for this.

Other works on the extrusion of semi-crystalline polymers, like PE [97,123] and PLA [98,99] have also reported increases in cell density with the talc concentration. In the work by Pilla [98] (2010), the addition of talc effectively reduces up to 3 times the cell size of PLA and PLA/PBAT foams blown with CO_2, increasing the cell density of the

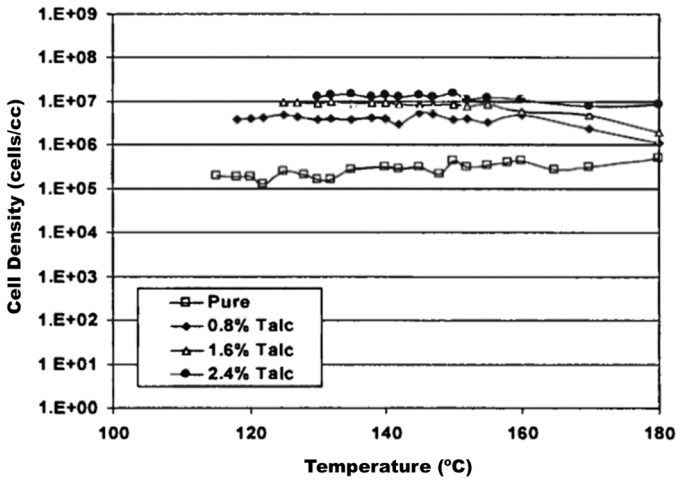

Fig. 9. Effect of talc on cell nucleation of PP foam blown with 10 wt% butane, from reference [122], reproduced with permission.

materials. It also increases crystallinity and has a diminishing effect on the open-cell content of the foams. A later work by Nofar [99] et al. found that, up to a certain content (0.5 wt%), talc works as efficiently as other nucleants with smaller particle sizes and higher surface area. This is attributed to a stronger effect of talc in the acceleration of the crystallization dynamics, creating crystals that appear sooner, which work as heterogeneous nucleants.

3.3.2. *Clays and silicas*

Clays and silica particles are often used as nucleating agents in foaming processes. Like talc, both are inorganic, mineral-based particles with relatively high surface areas that don't react with the polymer matrix and can have a wide variety of shapes and surface chemistries. The difference between these particles and talc is the much higher surface area and usually smaller particle size of clays and silicas compared to talc particles, which makes them potentially much more efficient nucleating agents. As listed in Table 1, while clays usually have a platelet shape with very high aspect ratios, silica particles have a great surface area but a rather spherical overall shape. Their small particle sizes make them effective heterogeneous nucleation sites. However, due to their intrinsic hydrophilic nature, dispersion within the hydrophobic polymeric phase is often poor [100]. For this reason, surface treatment or chemical modification is commonly employed to improve compatibility and achieve uniform dispersion. Clays used in polymer nanocomposites are most often layered aluminosilicates, typically montmorillonite, consisting of tetrahedral silicate (SiO_4) sheets and octahedral aluminate (Al^{3+}) sheets (sometimes substituted by magnesium (Mg^{2+})) arranged in a high aspect ratio layered structure. In contrast, silicas are generally amorphous silicon dioxide (SiO_2) particles with large specific surface areas and abundant surface silanol (Si-OH) groups, which make them highly hydrophilic but also highly tunable through surface functionalization [26,124,125].

One of the earliest works using clays in extrusion foaming was conducted by Han [100], who studied the effect of different contents of Cloisite 20 A (a montmorillonite clay) in a polystyrene matrix. The work studies the difference between direct mechanical blending of the PS and the clay in the extruder and a previous surface modification combined

with in situ polymerization in order to obtain exfoliated PS-clay nanocomposites. The CO_2-blown extrusion gives high-density foams (around 700 kg/m^3) in which the nucleating effect of the clays can be clearly observed, as cell density in the composites is higher than in the pure polymer in all cases. Mechanical blending of the Cloisite 20 A particles with polystyrene causes a cell size reduction from 25 to 11 μm, while the modified and in-situ polymerized composites reach 5 μm, in both cases with a clay content of 5 wt%. Fig. 10 shows a picture comparing these two PS/Cloisite 20 A foams with one containing 5 wt% talc. In another work by Zhang [81] where they compare several nucleating agents in order to obtain bimodal cellular structures, the PS composites with a 1 wt% content of platelet-like nanoclay Cloisite 30B achieve the bigger cell size reduction, of around ten times (from 740 to 60 μm) in extruded foams blown with CO_2 and H_2O, obtaining a unimodal, highly homogeneous cellular structure. The nucleating effect of nanoclays in PS has been further analyzed in works with other foaming methods, as injection molding [126] and batch foaming [127,128].

Zhai et al. [103] studied the effect of Cloisite 20 A in polypropylene extruded with CO_2. They used maleic anhydride grafted polypropylene as a coupling agent. As in other previous cases, cell density was found to increase and cell size to decrease with the content of nucleating agent, finding the biggest step between the pure polymer and the composite with 0.5 wt% Cloisite 20 A, with a dramatic cell density increase of two orders of magnitude (from 10^5 to 10^7 cells/cm^3). The work explores a range of die temperatures (130–150 °C), and at all temperatures the variation of cell density with the additive content was similar, while, for a fixed additive content, cell density decreases slightly with temperature. Also, the foaming window was seen to widen with the dispersed clays in the matrix thanks to an enhancement of melt viscosity. Also, the crystallinity was affected by clay particles, as their presence induced a higher number of smaller crystals, which plays a part in the nucleation increase. Despite clays decreasing cell size and increasing cell density at the lowest content, homogeneity of the structure is very poor until a 2 wt % content is reached, and optimum when using a 5 wt%.

In a work from 2016, Wang [129] studied PP/PS blends for bimodality, analyzing both pure polymers and various blends with PS contents ranging from 10 to 40 wt% and repeating the experiments with a 1 wt% content of clay. Without the clays, all the blends gave a bimodal cellular structure where the bigger cells appeared in the polystyrene phase of the blend. When introducing the nucleating agent, not only did cell density increase, but bimodality disappeared, and the average cell size was reduced (approximately by half in the pure polymers) due to the particles dominating the nucleation process.

Silica particles are less studied than clays, especially in amorphous polymers. In fact, only one work on polystyrene was found using the extrusion foaming technique [82]. They used untreated silica particles and found that an increasing content of particles (0, 1, and 3 wt%) reduced cell size and enhanced nucleation.

Lee et al. [118] studied the dispersion of SiO_2 particles in a PP matrix in a compound extrusion prior to the extrusion foaming, and later they reproduced the formulations in a foaming extruder with CO_2 as the blowing agent. They found that nucleation was enhanced by silica at concentrations less than 1 phr. From that concentration on, the size of the aggregates was too big to act as an efficient nucleating agent. This study highlights the importance of good particle dispersion to maximize the effect of the nucleating agent, which can be achieved through the optimization of the processing and pre-processing (pre-dispersion of the particles in a masterbatch compound) conditions.

A work by Zandi et al. [104] using nanoclays in LDPE blown with a mixture of n-butane and n-pentane reported the enhancement by the clays of other characteristics of the foam apart from the cellular structure. The cell density increased up to 2 times and cell size was reduced around 30%, increasing the homogeneity of the structure, also leading to foams with reduced thermal conductivity [130,131]. The Young's modulus of the blends is also higher than the pure PE foam, but it has a maximum at 0.3 wt% clay content, while when doubling the clay concentration, the modulus decreases due to a weakening induced by having too much additive in the polymer cell walls. On the other hand, it is proven that the clays in the polymer work as flame retardants.

Other works tried these nucleating agents in PLA as well. In a work by Matuana and Diaz [105], high density PLA foams are blown with CO_2. When adding nanoclays to the polymer, the microcellular structure, formed by pores of 3–5 μm, does not change significantly, but nanometric pores (100–200 nm) appear in the previously unfoamed areas. Fig. 11 shows images of the cellular material without (a and b) and with 5 wt% nanoclays (c and d). Fig. 11.d clearly shows a secondary

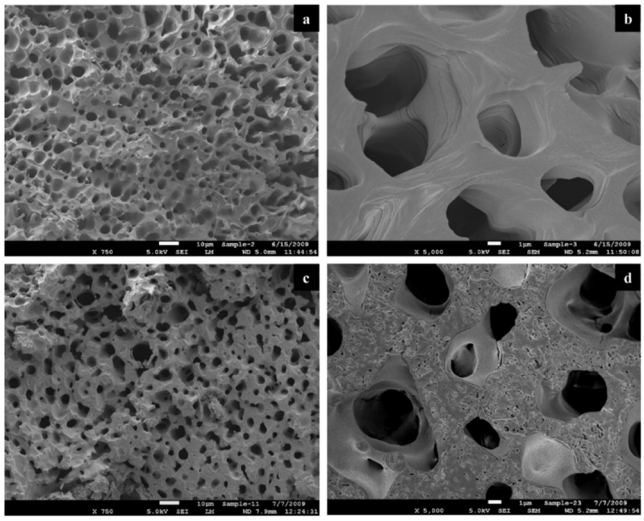

Fig. 11. SEM micrographs illustrating the effect of nanoclay addition on the cell morphology of semicrystalline PLA foams: (a and b) without nanoclay; (c and d) with nanoclay. Micrographs a and c were taken at low magnification (750×), whereas micrographs b and d were taken at high magnification (5000x), from reference [105], reproduced with permission.

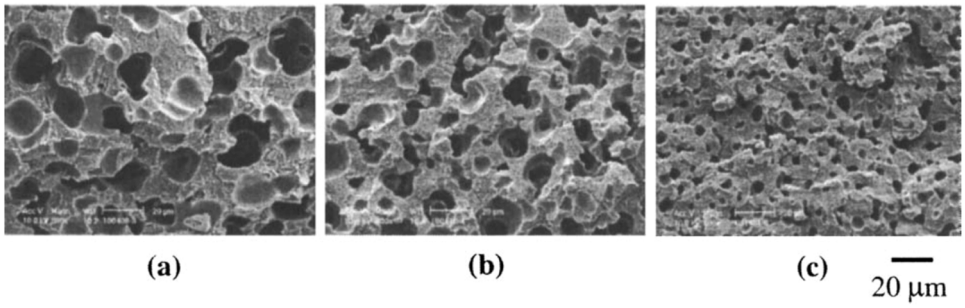

Fig. 10. SEM images of (a) PS/5 wt% talc, (b) PS/5 wt% Cloisite 20 A, and (c) PS/5 wt% MHABS (modified, exfoliated Cloisite 20 A), from reference [117], reproduced with permission.

nanocellular structure among the large pores. In this work, PLA pellets are ground prior to the blending in order to optimize the dispersion of the clay. Another work by Keshtkar et al. [102] stated the problem of the low melt strength and molecular weight drop of PLA during extrusion, which makes it difficult to obtain low-density foams and high cell densities. They proved that this issue can be prevented with the addition of nanoparticles instead of chain extenders, as it will be discussed in Section 4. In these experiments, several contents of nanoclay Cloisite 30B are added to the PLA matrix and cell size is reduced from 220 μm in the pure PLA to 60 μm in the blend with 5 wt% clay content, while density is also reduced from 55 to 30 kg/m^3. In a work by Nofar [99], nanosilicas and nanoclays are added to the PLA in contents of 0.5 and 1 wt%, and results are compared with samples using talc as an additive. While talc worked as well as the nano-additives at the lowest content due to talc inducing higher acceleration of crystallization kinetics, at 1 wt%, the effect of the nanoparticles clearly outperforms talc in both cases. Overall, the nanosilica and nanoclay particles improve the expansion ratio and cell density in the same amount and reduce cell sizes by more than 10 times with a concentration of 1 wt%.

Nucleating agents can also be helpful to easy the processing conditions to reach micro- and nanocellular foams. For instance, in the work of Costeux about the production of nanocellular PMMA by extrusion [90], they use nanosilica too to improve the processability of the system. While the cell size did not increase with the addition of the nanoparticles, they were able to obtain a similar foam at a lower concentration of CO_2 by adding 0.25 wt% of SiO_2.

3.3.3. *Carbon allotropes*

A significant number of studies have focused on the use of carbon-based materials as nucleating agents in extrusion foaming. These include carbon nanotubes (CNTs) or nanofibers (CNFs), graphite, and their derivatives (see Table 1). Owing to their high surface area, very small particle size, and mechanical strength, carbon-based fillers are particularly attractive for improving not only nucleation efficiency but also the overall performance of polymeric foams. Their ability to promote heterogeneous nucleation contributes to a more refined and uniform cell morphology in different foaming processes [132,133] while their inherent radiation absorbing properties can enhance the thermal insulation capacity of the foam [134]. Numerous works in the literature have explored the use of these materials, reporting often successful results regarding cell size reduction.

One of the first studies involving carbon nucleating agents in extrusion was carried out by Shen and coworkers [107]. In this work, they used nanometric CNFs (100 nm thick) both as a reinforcement and nucleant in PS extruded microcellular foams. The addition of 1 wt% CNFs reduced the cell size from 8.7 to 7.2 μm, while increasing the content to 5 wt% further decreased it to 4.1 μm (see Fig. 12). Furthermore, CNFs also improved the mechanical properties. Yet, densities of the foams in this work are quite high (600–700 kg/m^3), though it can be taken as a reference, as the effect of the carbon nanofibers content is clearly noticeable, reducing cell sizes to less than half the ones in the pure polymer foam.

In the work by Zhang et al. [101], several carbon-based nucleants are tried independently in PS using CO_2 as the main blowing agent with and without water as co-blowing agent. From the three different particles (activated carbon, CNFs and expanded graphite), samples with expanded graphite achieved a reduction in cell size of more than 300% with a concentration as low as 0.5 wt%, with a decrease from 275 μm in the pure polymer to 75 μm in the said composite foam. The other nucleants allowed cell size reductions to around half the size of the pure PS foam. The sample with the 0.5 wt% content of expanded graphite also has the lowest thermal conductivity value of this study. It is remarkable that, while achieving these reductions in cell size, all the foams produced in this work have densities below 50 kg/m^3. Okolieocha and coworkers [95] went one step further, using graphene (thermally reduced graphite oxide, TRGO) and comparing this nucleant to multi-walled carbon nanotubes (MWCNTs) and talc. Surface area of the TRGO particles is 3 times the surface area of the MWCNTs (650 vs 198 m^2/g, respectively) and more than 60 times the surface area of talc particles (12 m^2/g). TEM images of the foams containing 1 wt% of each additive are shown in Fig. 13. In this CO_2 extrusion process assisted with ethanol (EtOH), both carbon materials overperformed talc, as shown in Fig. 14. MWCNTs manage to reduce the cell size 6 times, while TRGO particles reduce cell size up to 16 times, from 400 μm of pure polystyrene to 25 μm with a content of 1 wt% nucleant, maintaining the density of the foam reasonably low (60 kg/m^3). This effect is attributed by the authors to two mechanisms: the highest surface area of TRGO particles and their flatter surfaces, with a lower contact angle with the physical blowing agent, which translates to a lower free energy barrier and higher nucleation. Furthermore, the particles can limit cell expansion and, subsequently, coalescence both by increasing the melt viscosity of the matrix and mechanically, acting as “barricades” to cell expansion in the cell walls and struts, also improving cell morphology homogeneity. In all cases, the compressive modulus and strength of the foams increased with increasing the additive content. In other work, Fei [106] uses MWCNTs again in PS with CO_2. In this case, the cell size is roughly halved with a 1 wt% content, very similar to the results with micro graphite (mGr), also employed in this work.

For polyolefins such as PP and PE, carbon allotropes have been reported to work well in other foaming technologies [135–137], but the research in extrusion foaming is quite scarce. In the work of Fasihi et al. [108] in 2016, a successful increase in nucleation is found in PP using expanded graphite as the nucleating agent. The experiments are made by extrusion with a chemical blowing agent (sodium carbonate or sodium carbonate and citric acid). A 1 wt% content of expanded graphite is proven to achieve smaller cells in all cases regarding the foams with 1 wt% content of talc (from 600 to 300 μm), also enhancing cell density by a factor of 10.

A wide research of foamed PET with MWCNTs and micrographite (mGr) is found in a 2020 study by Pan [116]. In this work, they study how two different contents of these nucleating agents affect the final properties of the HFC-blown extruded foam, including the crystallinity of the polymer. They showed that the particles added to the polymer not only increase the nucleation efficiency of the foaming process, but also

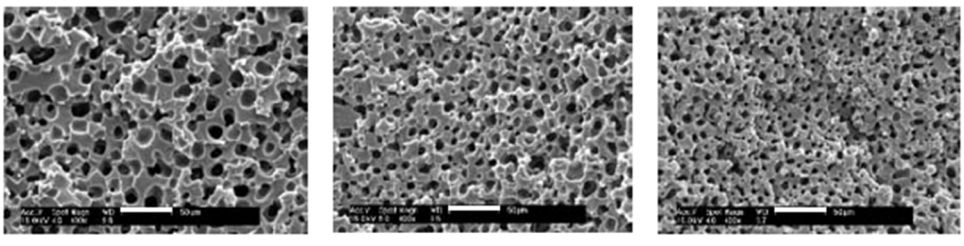

Fig. 12. PS/CNFs extruded foams under the same extruding conditions. (a) Pure PS, (b) PS – 1 wt% CNFs, (c) PS – 5 wt% CNFs, from reference [107], reproduced with permission.

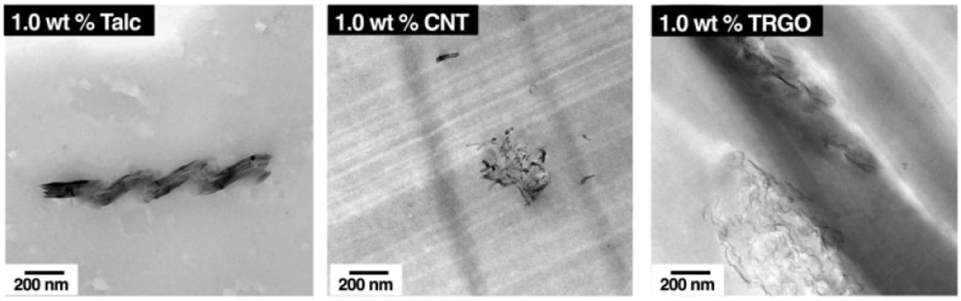

Fig. 13. TEM images of PS PS/1.0 wt% talc, CNTs, and TRGO foams [95].

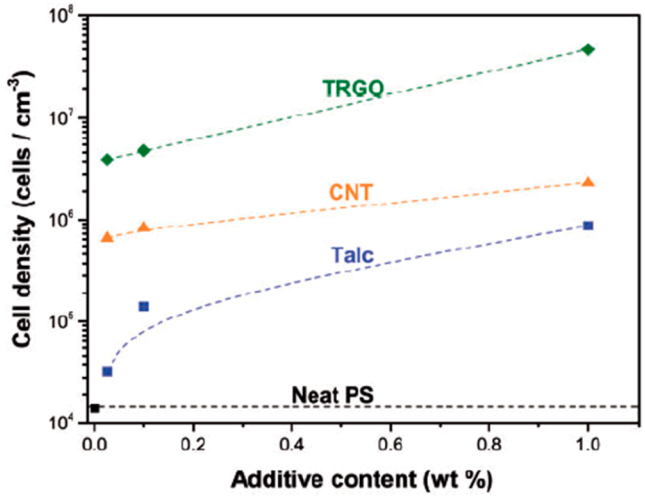

Fig. 14. Cell density as a function of additive content in extruded polystyrene foams [95].

promote crystallization, by raising the degree of crystallinity (by 50–100%) and halving crystallization half time. Also, a strong increase in the crystallization temperature with the content of the additive is found in both cases. In this context, cell nucleation and homogeneity are greatly impacted and improved both because of the effect of the particles and the higher number of crystals that can also act as nucleation sites for the cells of the foam. Also, these crystals can inhibit the excess of cell growth when they are large enough, preventing cell coalescence and hence increasing the homogeneity of the cellular structure. Between the two nucleating agents, MWCNTs give better results than mGr because of their higher surface area, giving a cell size reduction from 87 to 50 μm and a 4-time increase in cell density.

Overall, the use of carbonaceous particles as nucleating agents gives successful results, reducing the size of the cells in the extruded foams. Wider research has been done using these types of additives in batch foaming experiments, backing their use [6135,138,139]. The enhancement of the foam properties goes beyond nucleation, as these agents have been proven to contribute directly to reducing thermal conductivity through the scattering and absorption of infrared radiation [138, 140,141]. All these results make this type of nucleating agent a highly compelling topic for future research.

3.3.4. *Other particles used as nucleating agents*

While the most common nucleating agents found in the literature have been discussed in the previous sections, other studied particles also show remarkable results. For instance, Yu [109] used calcium carbonate ($CaCO_3$) in a PS matrix based on previous research conducted in batch foaming experiments with PS and PP [142,143]. In these extrusion experiments, nano-$CaCO_3$ particles coated with stearic acid were blended with PS in various contents and extruded with CO_2. The particle concentration had a strong correlation with cell size and cell density of the resulting foam, reducing the diameters of the cells from 310 μm of the pure PS to 54 μm with the blend with 5 wt% content. Increasing the content of $CaCO_3$ to 10 wt% induced a dramatic increase in cell density and a decrease in cell size (28.7 μm), but also affected the structure of the foam, making it open and non-uniform. When the content was further increased to 15 and 20 wt%, a bimodal structure appeared attributed by the authors to an uneven distribution of CO_2 during the foaming process: This occurs because supercritical CO_2 in the PS melt preferentially diffuses toward the heterogeneous nucleation sites, promoting cell growth, while the more stable nuclei do not overgrow and instead remain evenly dispersed within the cell walls.

Hydrocerol is a special nucleating agent that can be considered "active", as its particles promote heterogeneous nucleation, but it also decomposes with temperature, releasing water and CO_2. In fact, in most cases, it is used as the blowing agent in the process [144–146]. The working principle is based on the endothermic reaction between a carboxylic acid and a carbonate or bicarbonate salt that usually happens in the range of 160–220 °C. Special care needs to be taken with the pressure and temperature in the feed zone of the extruder to prevent gas loss through it due to early decomposition. Few studies have been found that analyze the nucleating effect of Hydrocerol in the extrusion of polymer foams with a physical blowing agent. An early study by Behravesh [144] with PP and isopentane showed that the hydrocerol had a nucleating effect up to a certain concentration (1 wt%) at which it started to govern nucleation. Kropp et al. [147] also found an optimum concentration above which no further improvement was seen. They did experiments with TPU, SEBS, and PP/EPDM and found that an increasing concentration of Hydrocerol (up to 0.5 wt%) increased the amount of nuclei and cells formed, and decreased cell size and foam density.

Table 3 summarizes the best results of the works reviewed regarding the use of nucleating agents. The table includes the percentage of cell size reduction in comparison to a reference system without the nucleating agent.

3.3.5. *Polymer blends*

As one can infer from reading this section, the most usual way to promote nucleation in polymer extrusion foaming processes is the addition of inorganic particles. Nevertheless, the addition of another polymeric phase to the matrix can also induce heterogeneous nucleation phenomena. Benzene-trisamides (BTAs) are another promising nucleating agent with very promising results. First tried in isotactic polypropylene (iPP) injection molding process, this additive self-assembles in the molten polymer in nanometric rod-like structures with high surface areas that enhance nucleation [148]. These first experiments managed to lower cell sizes up to 6 times (120–20 μm) with a content as low as 0.02 wt%. Consequently, three different types of BTAs were later used in iPP extrusion foaming with CO_2, achieving in all cases smaller cells than neat PP and PP with talc [149]. They also found that all the blends outperformed the neat PP sample in compressive modulus, an effect that the authors attributed to a mechanical reinforcement thanks

to the shape and position of the BTAs in the cell walls of the foam. In 2019, works by Aksit et al. [110,119] introduced this technique in polystyrene extrusion foaming blown with CO_2 and EtOH with the will of studying the effect of this nucleating agent in an amorphous polymer, and found great results in both cell size reduction and homogeneity enhancement of the cellular structure. Cell size was reduced from 632 μm of the pure PS foams to 18 μm of the blend with a 0.2 wt% content, increasing cell density by 5 orders of magnitude, with a foam density of 72 kg/m^3. With a higher concentration of 0.5 wt%, the cell size increases again, because of the amount of additive surpassing its solubility limit in PS at the processing conditions: at a concentration of 0.2 wt%, diameters of the BTA structures were in the range of 300 – 400 nm while for 0.5 wt% concentration, they grow to 500–600 nm, as shown in Fig. 15. This limitation also affected the compressive modulus of the samples, with the 0.2 wt% concentration being the optimal for its enhancement (+ 23% in the normalized compression modulus). The thermal conductivity of the samples was also improved in all cases by at least 10%.

Another work by Kun Wang et al. [112] blended polytetrafluoroethylene (PTFE) in a polypropylene matrix, obtaining a fibrillar structure, shown in Fig. 16, with nanometric diameters (300–500 nm) and lengths well above 100 μm, obtaining high aspect ratios. This is achieved by melting both polymers at a temperature (around 200 °C) that is between their melting temperatures (163 °C for PP and 342 °C for PTFE), but enough for the PTFE aggregates to elongate into those fibrillar structures during mechanical mixing. This work achieves a reduction in cell size from 300 to 141 μm (60 kg/m^3) with a PTFE concentration of 1 wt% and 110 μm with 4 wt% PTFE (100 kg/m^3).

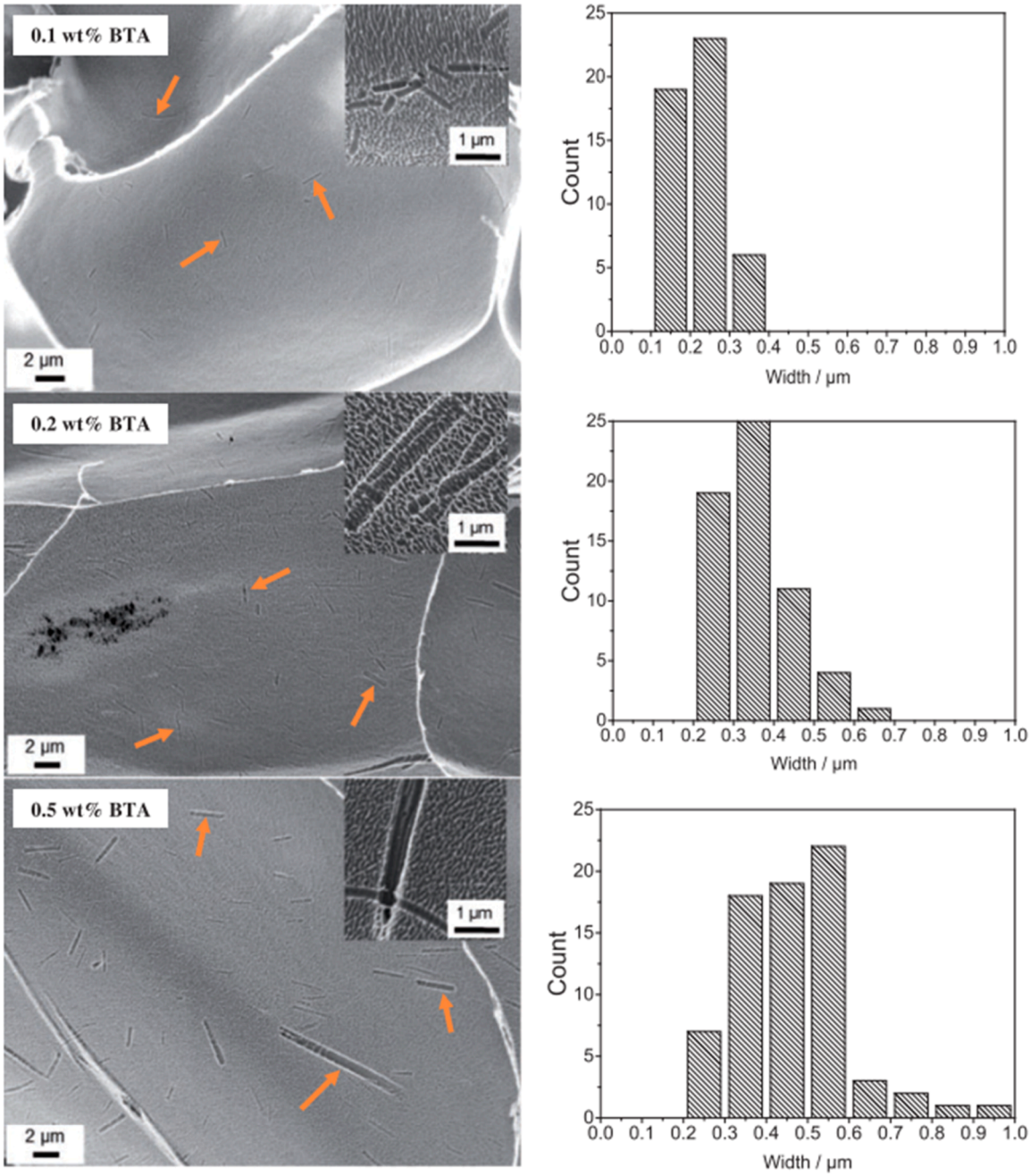

Fig. 15. SEM images of XPS with 0.1, 0.2, and 0.5 wt% BTA after 60 min plasma etching. Orange arrows and magnified insets reveal holes left by BTA nano-objects removed during plasma treatment. Hole-width histograms correspond to the BTA nano-object diameters, from reference [110], reproduced with permission.

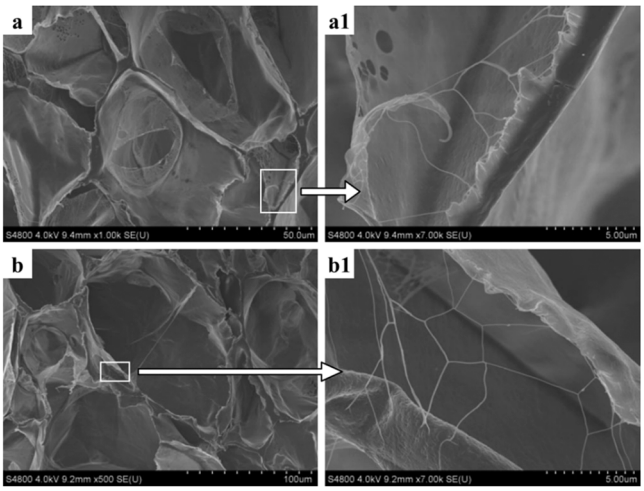

Fig. 16. Dispersion of PTFE in LPP/PTFE2.0 (a,a1) and LPP/PTFE4.0 (b,b1) foams, from reference [112], reproduced with permission.

They also found that the addition of the secondary polymer widened the foaming window on the higher end, thanks to the increased strain hardening provided by the fibrillar structure, and density was lower in the blends from a foaming temperature of around 158 °C. A subsequent study by Rizvi et al. [111] tried a lower PTFE concentration of 0.3 wt%, carrying out similar experiments. They concluded that the PTFE fibrils create a vast number of interfacial surfaces where the nucleation energy barrier was lowered, reducing the cell size from 225 to 48 μm. The fibrils also acted as CO_2 reservoirs and increased the strain hardening of the melt, allowing bigger expansions (density of the foamed blend is 32 kg/m^3). The foaming temperatures tested in these experiments were always lower than those used in the previous reference. In this case, the blend always had lower densities with respect to the pure polypropylene foams.

In other cases, the second polymeric phase does not need to be dispersed in a certain structure inside the matrix, but it is added in order to tune some property of the main polymeric matrix that needs to be adjusted to obtain a smaller structure. For example, Wang added different amounts of polyolefin elastomer (POE) to a PP matrix (mixed with wood flour and talc) and observed how the different concentrations of POE from 10 to 40 wt% enabled up to 58% cell size reduction (78 μm) by means of enhancing the melt strength of the blend [150].

4. Strategies for cell opening

The range of applications of extruded polymer foams can be further expanded by opening the cell walls. It is well known that open-cell foams in combination with flexible polymer matrices are the preferred choice for comfort applications thanks to their cushioning properties. In the case of rigid foams, while mechanical performance can be reduced, open-cell foams can be used for other purposes such as filtration [151], oil absorption [152], or acoustic absorption [153], among others. Also, the opening of the structure would allow the fabrication of a vacuum insulation panel (VIP), extracting all the air from inside the structure and reducing the thermal conductivity significantly [29,154], as has previously been noticed. The same complexity found for cell size control occurs with cell opening when it comes to extrusion: several parameters of the process are intertwined and obviously affect each other, affecting open-cell content along with cell size, density, etc. In this section, strategies found in the literature for producing open-cell extruded foams are discussed, trying to understand how the various mechanisms affect the outcome. Two main approaches have been identified in the literature: modification of the melt strength to modify viscosity and allow cell wall rupture (without compromising expansion), and addition of secondary phases that create weak points for cell wall rupture. Though the section is divided into two different approaches, they can often overlap (for instance, second phases can alter melt strength) – yet, the mechanisms are different.

4.1. Modification of the melt strength

Melt strength measures the tenacity of a given polymeric formulation at a certain temperature. It is well established that foaming requires melt strength: the formulation must be viscous enough to withstand the expansion without breaking the walls too soon [155]. Otherwise, gas will escape through the open structure, hindering further expansion. Extrusion processes are especially sensitive to this, since the expansion occurs at quite high temperatures at which the melt strength is, in general, low. In fact, many works focus on modification of the melt strength to assure good foaming (and typically, closed cell structures). For instance, PLA foaming is known to require a chain extender to create enough viscosity during expansion [156,157], and reactive foaming is used to increase the extensional viscosity of recycled PET [158,159].

Yet, it is possible to use melt strength as a tool to create open cells. The key is to achieve a compromise, and keep the cells closed during the expansion to achieve the density reduction, and only when a given cell wall thickness is reached, the cells would break.

PLA is usually linear, and open-cell structures are relatively easy to obtain. Some works have analyzed the influence of adding a chain extender, which was proven to increase the open-cell content [160] by introducing harder regions in the matrix. The use of the chain extender enhances nucleation and lowers the cell size and cell wall thickness, achieving, in some cases, foams with lower density and higher open-cell contents.

Lee et al. [161] developed a novel approach using cell wall thinning with polystyrene but went one step further by submerging the extrudate foam in cold water at the exit of the die, with the intention of inducing a big temperature difference between the solid skin of the sample and the inner structure. This way, the skin prevents the gas from escaping the foam, increasing pressure inside the cells and promoting a higher opening. Also, this method provides a longer preservation of high temperatures inside the foam, lowering the melt strength of the matrix. They compared this setup with a normal extrusion setup without cooling in the die, and tried several temperatures and pressure drops (through several die morphologies). The cooling setup was proven to provide higher open-cell content in most cases. For samples with 7 wt% CO_2, open-cell content was increased from 79 to 95% at the optimum temperature (155 °C) conditions. This temperature was found to be quite higher than the temperature for the maximum volumetric expansion (135 °C), finding that there is a compromise between the finer cell wall thickness at maximum expansion and a melt strength threshold at which the polymer starts to permit the breaking of the walls.

4.2. Addition of heterogeneities and use of polymer blends

The main mechanism or strategy to open the cell walls of a polymer in extrusion is based on the idea of introducing hard/soft inhomogeneities in the polymer matrix that cause the cell walls to break and open during the foaming process. Works by Park, Lee, et al. [45,151,162] studied this approach widely with LDPE. The basic idea, depicted in Fig. 17, is promoting the existence of nonuniform hard and soft regions through cross-linking at a high processing temperature, basing then the approach in developing specific, high melt strength regions in the matrix. During expansion, the cell walls start to break in the soft (non-cross-linked) areas as they get thinner, while the hard (cross--linked) regions maintain the cellular structure and avoid total coalescence. These studies show how the open-cell content of the foams grows with the cross-linking agent amount, up to a point where it creates excessive melt stiffness and is detrimental to foam expansion and thus to cell opening. The strategy can then be boosted by two methods. First, as

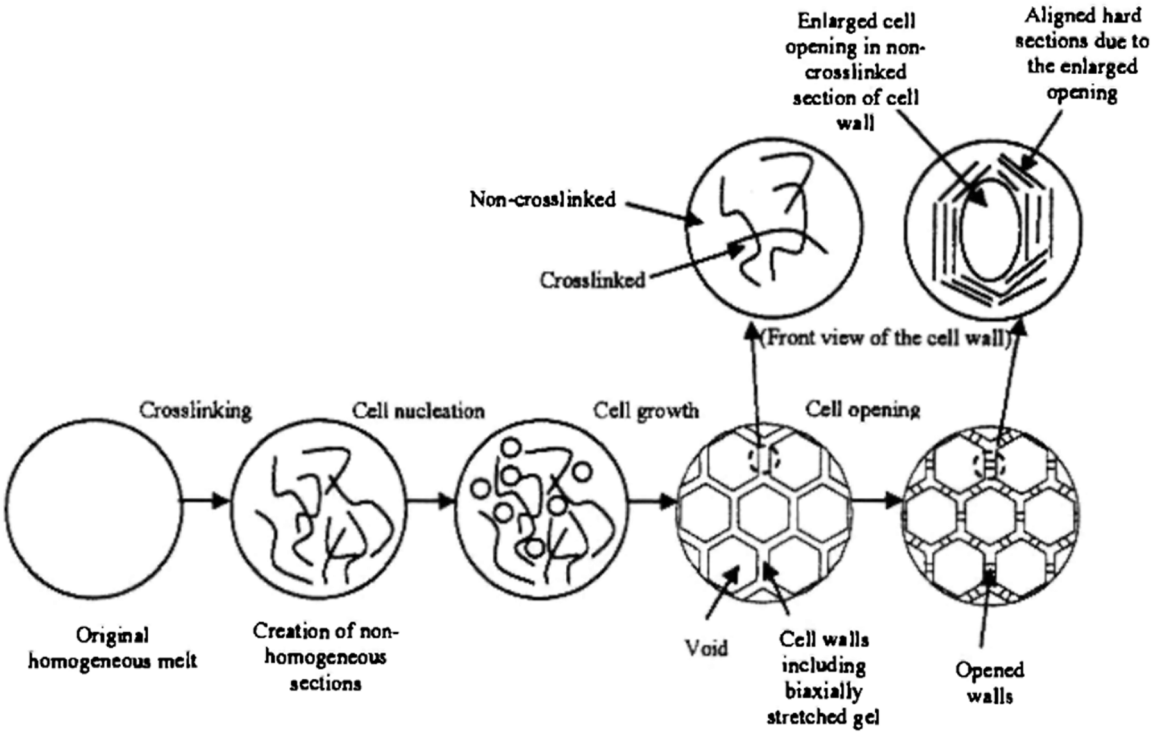

Fig. 17. Mechanisms for obtaining open-cell PE introducing cross-linked regions with improved melt strength, from reference [45], reproduced with permission.

the cell wall thickness is directly related to expansion, enhancing expansion has a positive effect on cell opening. In this scope, an optimal temperature should be found that, on one side, is high enough for the melt strength of the polymer to allow cell walls to break but, on the other side, is not too high to encounter a decrease in foam expansion. Fig. 17 shows the different mechanisms governing cell wall opening depending on the temperature of the process. A second way of reducing cell wall thickness is by promoting nucleation, as more cells in the same volume lead to thinner walls. In these works, PS and talc are added to PE and have been proven to improve the cell opening content. For example, at 110 °C, 10% PS increases open-cell content from 70 to 85%. Nevertheless, higher contents of PS seem to be worse for this purpose.

Also, a higher amount of CO_2 was seen to increase the open-cell content, as it has a positive effect on nucleation density, and thus, cell wall width was reduced. In one of the works, n-butane is added as a co-blowing agent and proven to enhance the temperature window at which high open-cell contents can be achieved. For samples LDPE/PS 90/10 blends (black circle in Fig. 18.b), 6 wt% butane makes 100% OC content achievable from 80 to 110 °C, and above 90% up to 140 °. This outcome is provided by a strong plasticization effect of butane, which provokes soft, non-cross-linked regions in the melt to break at lower temperatures, where the expansion of the material is higher.

Similar approaches have been made, but instead of creating the hard/soft heterogeneities with cross-linked and non-cross-linked regions, doing so by blending two polymers with different crystallization temperatures, such as PP and PE. A study by Lee [163] does so with two different PP/PE blends, one with linear PP and LDPE, and another one with high melt strength (HMS) branched PP and metallocene PE. The premise is that when the blend has a majority of the harder polymer (higher T_c), soft domains will break with the elongation of the walls during foaming. However, this methodology encountered some drawbacks, as it was seen that the volume expansion ratio decreased as the

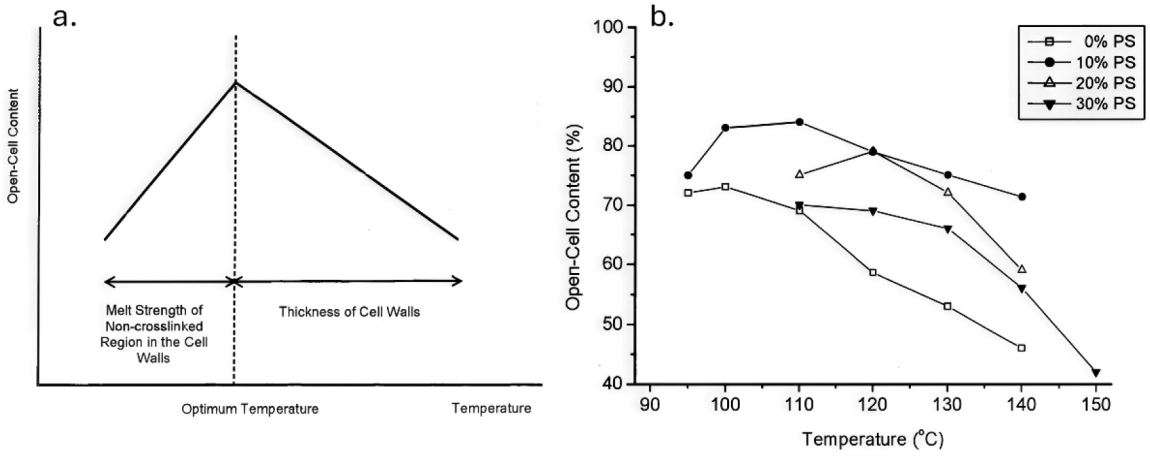

Fig. 18. (a) Mechanisms governing cell opening depending of temperature. (b) The Open-Cell Contents versus Die Temperature of LDPE-A/PS = 100/0, 90/10, 80/20, 70/30 with Crosslinking Agent Content 0.4% (8% C02, die L/D = 17.78 mm/1.016 mm), from reference [45], reproduced with permission.

second polymer amount increased, giving thicker cell walls despite a slight increase in cell density. On the other hand, if the dominant polymer in the blend is the one with the lower T_c, the two phases should debond when the wall thickness gets lower than the hard polymer domain. However, expansion ratios in this work are too low to prove this, probably because the extrusion temperature used was too high according to previously referenced studies on foaming polyethylene. Despite the premises, some of the best results are found with a homogeneous PP matrix, which is optimized in terms of processing temperature and pressure drop at the die (the higher, the better) to obtain close to 100% open-cell foams. This is because, at the temperatures used in this work, pure polypropylene foams can expand up to 30 times, achieving walls thin enough to break.

A work by Rizvi [164] employed PP blended with PTFE to achieve near−100% open-cell foams destined to oil absorption. As seen in the previous section, the PTFE takes the form of thin fibrils with less than 500 nm in diameter that enhance gas solubility, nucleation, and mechanical performance [111], achieving optimum open-cell contents. The PTFE fibrils will prevent the PP matrix from coalescing or collapsing. This way, higher cell density and bigger expansion ratios can be obtained, which has been proven to be crucial for high open-cell contents. The highest open-cell content achieved is 97.7% in a 70 kg/m^3 foam with a structure formed by mostly struts at 150 °C, which has been proven to be a very high temperature for processing PP alone. Instead of reinforcing PP, a softer phase can also be added, like POE, that has been proven to increase open-cell content of linear-PP from around 80 to more than 90% in studies by Wang and Pang [152,165].

Also, some studies explore the addition of a second polymer to PLA for cell opening purposes. For example, with the addition of poly (butylene succinate) (PBS) to PLA, a foam with more than 98% open-cell content and less than 30 kg/m^3 was obtained by Li et al. [166]. A work by Mihai [167] blended PLA with thermoplastic starch (TPS) at 50 wt%, finding a very interesting result: cell walls opened in very small holes (100 – 300 nm) in the walls, preserving the structural membrane of the walls, as seen in Fig. 19. A wide study by Chauvet et al. on PLA extrusion proved that 100% open-cell contents can be obtained for PLA extruded with CO_2 in a wide temperature window, from around 107–132 °C. Below 107 °, high expansion ratios were obtained, but melt strength did not allow cell opening [168]. Despite achieving 100% open-cell contents, homogeneous structures are not achieved at the same time.

5. Overview and future perspectives

Fig. 20 shows an overview of the results analyzed in this review. The results are presented in a cell size vs density graph that highlights the difficulties and lack of evidence found when trying to fabricate micro- and nanocellular polymer foams by extrusion foaming. As in some cases the foams are improved or modified without the use of any additive, pure polymers are depicted in the graph as darker points, and lighter ones represent polymers mixed with nucleating agents or other additives. It stands out that PP and PS materials (blue and green, respectively) are the most studied polymers in this foaming method, and low density foams are relatively easy to achieve. Also, it is clearly seen that the cell size of these materials can be significantly lowered when using nucleating agents. For instance, many works achieve reductions of cell size in PS of more than 90%. It also stands out that, while some PP foams with open cells are obtained through various techniques, only one partially open-cell PS foam is presented. PLA and PE foams are also represented in several studies. Results show that the same approaches used in PP or PS foams to reduce the cell size can be used in these other polymers, as well as the cell opening strategies used for opening the PP structure. Few studies were found with other polymers like PC or PET, but also showed interesting results.

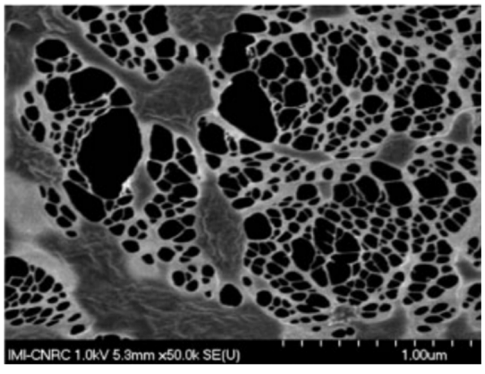

Fig. 19. Detail of the cell wall rupture in 50 wt% TPS/PLA foam, from reference [167], reproduced with permission.

As this extensive document reveals and is clearly seen in Fig. 20, very few works in extrusion foaming achieve cell sizes below 10 µm (microcellular range), and even less with open-cell structures, which limits the functionality and range of applications of extruded foams. In fact, it is shown in the graph that the region with cell sizes much lower than 10 µm and densities below 100 kg/m^3 lacks any points. Regarding nanocellular polymers (cell size below 1 µm), only one piece of evidence has been found, using PMMA, a polymer with a superior gas solubility compared with PS or PP, and a special extruder to withstand the extreme pressures needed. The intrinsic constraints -high temperatures, limited pressure range, short foaming times- present challenges in the control of the process when determined characteristics are looking to be improved or enhanced. An increase in nucleation and reduction in cell size usually has a counterpart in a lower expansion ratio (higher foam density), and while works in the literature show that both things can be achieved up to some extent with good control and knowledge of the process, when very low cell sizes are targeted, the challenge is more complex. Furthermore, combining cells in the said range and low densities with open structures is even harder, as the opening of the cellular structure needs to be carefully controlled so it does not prevent foam expansion or lead to coalescence and degeneration of the structure.

Within this context lie the challenges that would permit the industrial-scale viability of foams with these combined characteristics. Overcoming these challenges will require an even deeper understanding of the coupled effects of nucleation, cell growth, and stabilization under extrusion-relevant conditions, where high temperatures, limited pressure drops, and short residence times strongly constrain structural control. Future progress is therefore expected to rely on improved process design, monitoring, modelling, etc., and other developments like nucleating agents with enhanced functionalities. In-situ monitoring techniques and data-driven/AI modeling may provide the predictive capability needed to design processes with higher precision and efficiency. The use of machine learning and artificial intelligence can be very useful to help develop new strategies and models that predict the performance of the process. In fact, it has already been applied [169] to develop a forecasting model in the extrusion of PLA. Development of in-line characterization techniques and mechanisms that provide real-time control of the extrusion process would also help the fine tuning of the produced foams. Furthermore, the integration of advanced machinery that enables more demanding processing conditions has proven to be very promising. Technological innovations that allow very high pressures at an industrial scale and optimized die geometries are expected to expand the current limits of achievable cell size. The development of new nucleating agents with advanced and diverse functionalities, like surface engineering or self-assembly capability, could also be of great use and is already being applied in other foaming processes [170–172]. Surface-engineered or self-assembling additives can enable simultaneous control over nucleation, cell growth, and wall opening. Finally, the transition to sustainable and low-GWP blowing agents, together with bio-based or recyclable polymers, will ensure that progress in cell morphology control aligns with environmental imperatives.

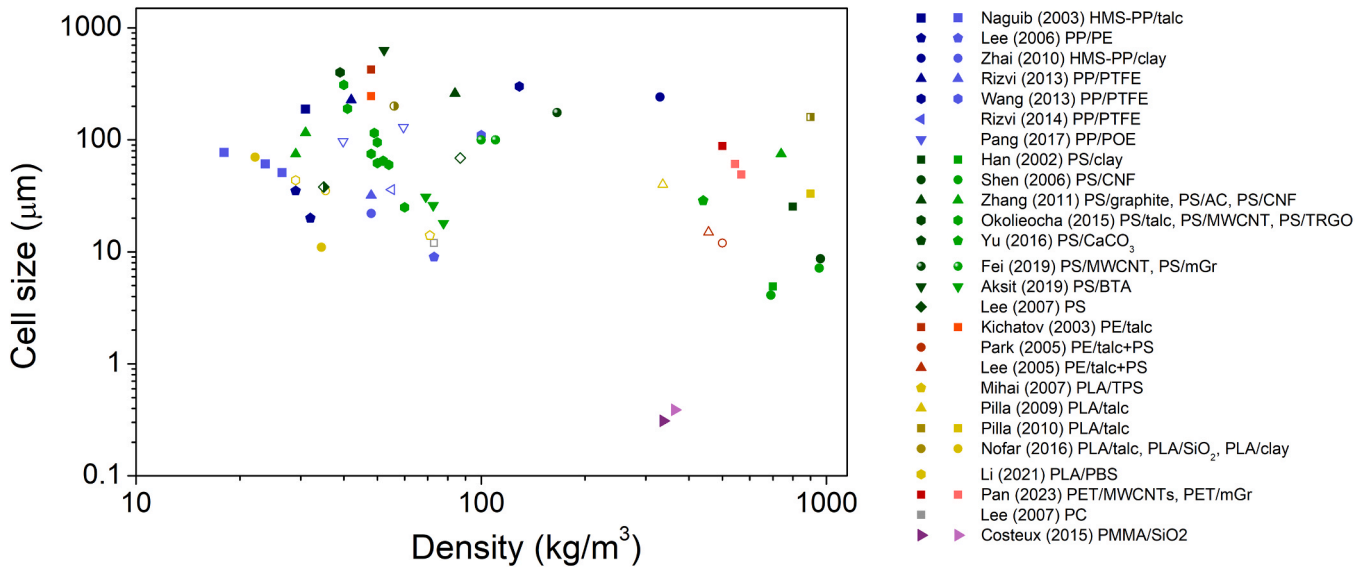

Fig. 20. Cell size vs density of some of the foams referenced in this work. Empty symbols mean open-cell (above 85%) and half-empty ones mean indeterminate of intermediate (30–85%) open-cell content and closed symbols represent closed cells. In two-color groups, the darker one stands for the pure polymer and the lighter for the polymer + additive.

6. Conclusions

This review has highlighted the difficulties of cellular structure control in extrusion processes to obtain light foams with low cell sizes (in the micro- and nanocellular range) and interconnected pores. As demonstrated through the review, this cannot be achieved through single-parameter optimization, but needs a multifactorial approach. Beyond the adequate processing parameters, formulation plays a major part in reaching those low cell size regimes. The polymer of choice and appropriate blowing or co-blowing agent influence not only the achievable cellular structure and density but also the environmental and operational feasibility of the process. Co-blowing strategies have been proven effective in widening the foaming window and improving structural homogeneity. Nevertheless, the most consistent advances in cell size reduction come from the incorporation of solid nucleating agents. Inorganic particles such as talc, nanoclays, and silicas, and carbon-based materials like graphene, carbon nanotubes, or expanded graphite, can significantly enhance heterogeneous nucleation and reduce cell diameter. Their effects extend beyond nucleation efficiency, often improving mechanical performance and cell uniformity by modifying melt viscosity and crystallization kinetics. However, dispersion quality, particle–polymer compatibility, and the competing influence of viscosity on expansion can limit their application to some extent. Besides the materials used, it has been found that the characteristics of the machine can be key to achieving very small cell size foams. Equipment with the possibility of reaching high pressures in the die (well above 20 MPa) has been proven to strongly enhance nucleation, but scalability would present some engineering and energetic challenges.

The transition from closed- to open-cell morphologies introduces further complexity, as the simultaneous reduction of cell size and increase in cell interconnectivity require opposing conditions. Thin cell walls and moderate viscosity are desirable for wall rupture, while high melt strength is needed to prevent structural collapse. A fine adjustment of process parameters (e.g., controlled pressure drop rate, die temperature profile) is needed to locate cell wall rupture where all nucleation and cell growth have already taken place, and yet do it without promoting cell coalescence.

Overall, it was seen that it is especially complex to obtain low-density materials with small cell diameters in the range of a few (< 10) microns. Furthermore, adding the goal of achieving open, interconnected structures makes the challenge even harder, as has been previously stated. If these challenges are overcome, new applications could be developed, like the large-scale production of Vacuum Insulation Panels or very high-absorbing materials for water purification.

CRediT authorship contribution statement

Judith Martín-de León: Writing – review & editing, Supervision. **Miguel Ángel RodrÍguez-PÉrez:** Writing – review & editing, Funding acquisition. **Marcos Merillas:** Writing – original draft, Investigation. **Victoria Bernardo:** Writing – review & editing, Writing – original draft, Supervision, Methodology, Conceptualization.

Declaration of Competing Interest

The authors declare the following financial interests/personal relationships which may be considered as potential competing interests: Miguel Angel Rodriguez-Perez reports financial support was provided by Spain Ministry of Science Innovation and Universities. Miguel Angel Rodriguez-Perez reports financial support was provided by Spain Ministry of Science Innovation and Universities. If there are other authors, they declare that they have no known competing financial interests or personal relationships that could have appeared to influence the work reported in this paper.

Acknowledgements

Financial support from grant PID2024–157392OB-I00 funded by MICIU/AEI/ 10.13039/501100011033 and, by "ERDF/EU" and grant PDC2025–165502-I00 funded by MICIU/AEI/ 10.13039/501100011033 and, by the "European Union NextGenerationEU/PRTR" are gratefully acknowledged.

Data availability

Data will be made available on request.

References

[1] R.S. Lakes, Cellular solids, J. Biomech. 22 (1989) 397, https://doi.org/10.1016/0021-9290(89)90056-0.
[2] D. Eaves, Handbook of Polymer Foams, Rapra Technology Limited Shawbury,, 2004.

[3] V. Kumar, N.P. Suh, A process for making microcellular thermoplastic parts, Polym. Eng. Sci. 30 (1990) 1323–1329, https://doi.org/10.1002/pen.760302010.

[4] J.A. Reglero Ruiz, M. Pedros, J.M. Tallon, M. Dumon, Micro and nano cellular amorphous polymers (PMMA, PS) in supercritical CO_2 assisted by nanostructured CO_2-philic block copolymers - One step foaming process, J. Supercrit. Fluids 58 (2011) 168–176, https://doi.org/10.1016/j.supflu.2011.04.022.

[5] I. Khan, D. Adrian, S. Costeux, A model to predict the cell density and cell size distribution in nano-cellular foams, Chem. Eng. Sci. 138 (2015) 634–645, https://doi.org/10.1016/j.ces.2015.08.029.

[6] G. Gedler, M. Antunes, J.I. Velasco, Effects of graphene nanoplatelets on the morphology of polycarbonate-graphene composite foams prepared by supercritical carbon dioxide two-step foaming, J. Supercrit. Fluids 100 (2015) 167–174, https://doi.org/10.1016/j.supflu.2015.02.005.

[7] D. Raps, N. Hossieny, C.B. Park, V. AltstÄdt, Past and present developments in polymer bead foams and bead foaming technology, Polym. (Guildf.) 56 (2015) 5–19, https://doi.org/10.1016/j.polymer.2014.10.078.

[8] J. Xu, Microcellular Injection Molding, John Wiley and Sons Inc,, 2010.

[9] J. Jiang, Z. Li, H. Yang, X. Wang, Q. Li, L.S. Turng, Microcellular injection molding of polymers: a review of process know-how, emerging technologies, and future directions, Curr. Opin. Chem. Eng. 33 (2021) 100694, https://doi.org/10.1016/j.coche.2021.100694.

[10] Extruded Polystyrene Market Size & Share Analysis - Growth Trends & Forecasts (2025 - 2030) Source: https://www.mordorintelligence.com/industry-reports/extruded-polystyrene-market, (n.d.). ⟨https://www.mordorintelligence.com/industry-reports/extruded-polystyrene-market⟩.

[11] J.E. Martini, The production and analysis of microcellular foam. Diss. Massachusetts Institute of Technology, 1981, Massachusetts Institute of Technology,, 1981.

[12] M.A. RodrÍguez PÉrez, J. Martín de LeÓn, V. Bernardo GarcÍa, Nanocellular Polymers, De Gruyter,, 2023, https://doi.org/10.1515/9783110756135.

[13] M. Shimbo, I. Higashitani, Y. Miyano, Mechanism of strength improvement of foamed plastics having fine cell, J. Cell. Plast. 43 (2007) 157–167, https://doi.org/10.1177/0021955×06075585.

[14] M.N. Bureau, V. Kumar, Fracture toughness of high density polycarbonate microcellular foams, J. Cell. Plast. 42 (2006) 229–240, https://doi.org/10.1177/0021955×06063512.

[15] V. Kumar, M. VanderWel, J. Weller, K.A. Seeler, Experimental characterization of the tensile behavior of microcellular polycarbonate foams, J. Eng. Mater. Technol. Trans. ASME 116 (1994) 439–445, https://doi.org/10.1115/1.2904310.

[16] R. Hasanzadeh, T. Azdast, A. Doniavi, M. Rostami, A prediction model using response surface methodology based on cell size and foam density to predict thermal conductivity of polystyrene foams, Heat. Mass Transf. Und Stoff. 55 (2019) 2845–2855, https://doi.org/10.1007/s00231-019-02628-8.

[17] B. Notario, J. Pinto, M.A. Rodriguez-Perez, Nanoporous polymeric materials: a new class of materials with enhanced properties, Prog. Mater. Sci. 78–79 (2016) 93–139, https://doi.org/10.1016/j.pmatsci.2016.02.002.

[18] B. Notario, J. Pinto, E. Solorzano, J.A. De Saja, M. Dumon, M.A. RodrÍguez-PÉrez, Experimental validation of the Knudsen effect in nanocellular polymeric foams, Polymers 56 (2015) 57–67, https://doi.org/10.1016/j.polymer.2014.10.006.

[19] G. Wang, J. Zhao, L.H. Mark, G. Wang, K. Yu, C. Wang, C.B. Park, G. Zhao, Ultra-tough and super thermal-insulation nanocellular PMMA/TPU, Chem. Eng. J. 325 (2017) 632–646, https://doi.org/10.1016/j.cej.2017.05.116.

[20] J. MartÍn-de LeÓn, J.L. Pura, V. Bernardo, M.Á. RodrÍguez-PÉrez, Transparent nanocellular PMMA: characterization and modeling of the optical properties, Polym. (Guildf.) 170 (2019) 16–23, https://doi.org/10.1016/j.polymer.2019.03.010.

[21] B. Notario, J. Pinto, M.A. RodrÍguez-PÉrez, Towards a new generation of polymeric foams: PMMA nanocellular foams with enhanced physical properties, Polym. (Guildf.) 63 (2015) 116–126, https://doi.org/10.1016/j.polymer.2015.03.003.

[22] S. Costeux, CO 2 -blown nanocellular foams, J. Appl. Polym. Sci. 131 (2014), https://doi.org/10.1002/app.41293.

[23] A.S. Zalusky, R. Olayo-Valles, J.H. Wolf, M.A. Hillmyer, Ordered nanoporous polymers from polystyrene-polylactide block copolymers, J. Am. Chem. Soc. 124 (2002) 12761–12773, https://doi.org/10.1021/ja0278584.

[24] C. Du Fresne Von Hohenesche, D.F. Schmidt, V. SchÄdler, Nanoporous melamine - Formaldehyde gels by microemulsion templating, Chem. Mater. 20 (2008) 6124–6129, https://doi.org/10.1021/cm8015319.

[25] J. MartÍn-de LeÓn, V. Bernardo, M.Á. RodrÍguez-PÉrez, Key production parameters to obtain transparent nanocellular PMMA, Macromol. Mater. Eng. 302 (2017) 3–7, https://doi.org/10.1002/mame.201700343.

[26] S. Liu, B. Zoetebier, L. Hulsman, Y. Zhang, J. Duvigneau, G.J. Vancso, Nanocellular polymer foams nucleated by core-shell nanoparticles, Polym. (Guildf.) 104 (2016) 22–30, https://doi.org/10.1016/j.polymer.2016.09.016.

[27] C. Canal, R.M. Aparicio, A. VÍlchez, J. Esquena, M.J. García-Celma, Drug delivery properties of macroporous polystyrene solid foams, J. Pharm. Pharm. Sci. 15 (2012) 197–207, https://doi.org/10.18433/j3×884.

[28] D. Cuadra-RodrÍguez, S. Barroso-Solares, E. Laguna-GutiÉrrez, M.Á. RodrÍguez-PÉrez, J. Pinto, Opening pores and extending the application window: open-cell nanocellular foams, Macromol. Mater. Eng. 308 (2023) 1–11, https://doi.org/10.1002/mame.202300087.

[29] F.A. Almeida, H. Beyrichen, N. Dodamani, R. Caps, A. MÜller, R. Oberhoffer, Thermal conductivity analysis of a new sub-micron sized polystyrene foam, J. Cell. Plast. 57 (2021) 493–515, https://doi.org/10.1177/0021955×20943101.

[30] G. Munters, J. Tandberg, 2,023,204 U.S. Patent, 2023204, 1935.

[31] S.-T. Lee, Foam Extrusion, Principles and Practice, CRC Press LLC,, 2000.

[32] A. Echte, F. Haaf, J. Hambrecht, Half a century of polystyrene-a survey of the chemistry and physics of a pioneering material, Angew. Chem. Int. Ed. Engl. 20 (1980) 344–361, https://doi.org/10.1002/anie.198103441.

[33] F.L. Johnson, 2,256,483 U.S. Patent, 2256483, 1941.

[34] R.G. Parrish, 3,637,458 U.S. Patent, 3637458, 1972.

[35] K. Cink, J.C. Smith, J.F. Nangeroni, J.R. Randall, 8,013,031 B2 U.S. Patent, 8013031, 2011.

[36] Extruded Polystyrene Market Research Report Information By Application (foundation, wall, roof, ceiling, floor, and others), by End-Use (Residential Construction and Commercial Construction), And By Region (North America, Europe, Asia-Pacific, And Rest Of, (n.d.). ⟨https://www.marketresearchfuture.com/reports/extruded-polystyrene-market-7500⟩.

[37] Polyethylene Foam Market Size & Share Analysis - Growth Trends & Forecasts (2025 - 2030) Source: https://www.mordorintelligence.com/industry-reports/polyethylene-foam-market, (n.d.). ⟨https://www.mordorintelligence.com/industry-reports/polyethylene-foam-market⟩.

[38] K.A. Ter-Zakaryan, A.D. Zhukov, I.V. Bessonov, E.Y. Bobrova, T.A. Pshunov, K. T. Dotkulov, Modified polyethylene foam for critical environments, Polymers 14 (2022) 4688, https://doi.org/10.3390/polym14214688.

[39] Extruded Polypropylene (XPP) Foam Market Size & Share Analysis - Growth Trends & Forecasts (2025 - 2030) Source: https://www.mordorintelligence.com/industry-reports/extruded-polypropylene-xpp-foam-market, (n.d.). ⟨https://www.mordorintelligence.com/industry-reports/extruded-polypropylene-xpp-foam-market⟩.

[40] M. Xanthos, Recycling of the #5 Polymer, Science (80–.). 337 (2012) 700–702. https://doi.org/10.1126/science.1221806.

[41] J. Wang, Q. He, S. Huang, Y. Cheng, H. Li, D. Chen, Mechanical recycling and performance characterisation of insert-injection moulded homo-polypropylene single-polymer composites and foams, Compos. Commun. 53 (2025) 102176, https://doi.org/10.1016/j.coco.2024.102176.

[42] S. Pilla, Handbook of Bioplastics and Biocomposites Engineering Applications, John Wiley & Sons, Inc,, Hoboken, NJ, USA, 2011.

[43] C. Vannini, F. Fiordelisi, W. Movilli, F. Lanzani, Polylactic acid-based degradable foams and process for their production, EP 1528079 A1, 2005.

[44] H. Zhang, Scale-Up of Extrusion Foaming Process for Manufacture of Polystyrene Foams Using Carbon Dioxide, University of Toronto, 2010.

[45] C.B. Park, V. Padareva, P.C. Lee, H.E. Naguib, Extruded open-celled LDPE-based foams using non-homogeneous melt structure, J. Polym. Eng. 25 (2005) 239–260, https://doi.org/10.1515/POLYENG.2005.25.3.239.

[46] J. Reignier, R. Gendron, Mechanical anisotropy of PS/CO_2 microcellular foam sheet prepared by foaming extrusion, J. Cell. Plast. 54 (2018) 87–101, https://doi.org/10.1177/0021955×16670586.

[47] C. Kwag, C.W. Manke, E. Gulari, Rheology of molten polystyrene with dissolved supercritical and near-critical gases, J. Polym. Sci. Part B Polym. Phys. 37 (1999) 2771–2781, https://doi.org/10.1002/(SICI)1099-0488(19991001)37:19<2771::AID-POLB6>3.0.CO;2-9.

[48] M. Sauceau, J. Fages, A. Common, C. Nikitine, E. Rodier, New challenges in polymer foaming: a review of extrusion processes assisted by supercritical carbon dioxide, Prog. Polym. Sci. 36 (2011) 749–766, https://doi.org/10.1016/j.progpolymsci.2010.12.004.

[49] W.-C.V. Wang, E.J. Kramer, Effects of high-pressure CO_2 on the glass transition temperature and mechanical properties of polystyrene, J. Polym. Sci. Polym. Phys. Ed. 20 (1982) 1371–1384, https://doi.org/10.1002/pol.1982.180200804.

[50] Z. Zhang, Y.P. Handa, CO_2-assisted melting of semicrystalline polymers, Macromolecules 30 (1997) 8505–8507, https://doi.org/10.1021/ma9712211.

[51] L. Lombardi, D. Tammaro, Effect of polymer swell in extrusion foaming of low-density polyethylene, Phys. Fluids 33 (2021), https://doi.org/10.1063/5.0035033.

[52] F. Rindfleisch, T.P. Dinoia, M.A. Mchugh, Solubility of polymers and copolymers in supercritical CO 2, J. Phys. Chem. 100 (1996) 15581–15857, https://doi.org/10.1021/jp9615823.

[53] Y. Sato, M. Wang, S. Takishima, H. Masuoka, T. Watanabe, Y. Fukasawa, Solubility of butane and isobutane in molten polypropylene and polystyrene, Polym. Eng. Sci. 44 (2004) 2083–2089, https://doi.org/10.1002/pen.20213.

[54] Y. Sato, M. Yurugi, K. Fujiwara, S. Takishima, H. Masuoka, Solubilities of carbon dioxide and nitrogen in polystyrene under high temperature and pressure, Fluid Phase Equilib. 125 (1996) 129–138, https://doi.org/10.1016/S0378-3812(96)03094-4.

[55] Y. Sato, T. Takikawa, S. Takishima, H. Masuoka, Solubilities and diffusion coefficients of carbon dioxide in poly(vinyl acetate) and polystyrene, J. Supercrit. Fluids 19 (2001) 187–198, https://doi.org/10.1016/S0896-8446(00)00092-9.

[56] V. Bernardo, Production and Characterization of Nanocellular Polymers Based on Nanostructured PMMA Blends and PMMA Nanocomposites, University of Valladolid,, 2019.

[57] S.-T. Lee, Polymeric Foams, CRC Press LLC,, 1985.

[58] C. Yang, M. Wang, Z. Xing, Q. Zhao, M. Wang, G. Wu, A new promising nucleating agent for polymer foaming: effects of hollow molecular-sieve particles on polypropylene supercritical CO_2 microcellular foaming, RSC Adv. 8 (2018) 20061–20067, https://doi.org/10.1039/c8ra03071e.

[59] L. Chen, D. Rende, L.S. Schadler, R. Ozisik, Polymer nanocomposite foams, J. Mater. Chem. A 1 (2013) 3837–3850, https://doi.org/10.1039/c2ta00086e.

[60] V. Bernardo, J. Martin-de Leon, J. Pinto, T. Catelani, A. Athanassiou, M. A. Rodriguez-Perez, Low-density PMMA/MAM nanocellular polymers using low MAM contents: Production and characterization, Polym. (Guildf.) 163 (2019) 115–124, https://doi.org/10.1016/j.polymer.2018.12.057.

[61] V. Bernardo, J. Martin-de Leon, E. Laguna-Gutierrez, T. Catelani, J. Pinto, A. Athanassiou, M.A. Rodriguez-Perez, Understanding the role of MAM molecular weight in the production of PMMA/MAM nanocellular polymers, Polym. (Guildf.) 153 (2018) 262–270, https://doi.org/10.1016/j.polymer.2018.08.022.

[62] E. Laguna-Gutierrez, Understanding the Foamability of Complex Polymeric Systems By Using Extensional Rheology, 2016.

[63] Y. Fukasawa, T. Okuda, T. Shimada, M. Hattori, H. Saito, Mechanism of permeability modification in polyethylene foams, J. Cell. Plast. 44 (2008) 107–123, https://doi.org/10.1177/0021955×07081649.

[64] J.B. Burkholder, O. Hodnebrog, B.C. McDonald, V. Orkin, V.C. Papadimitriou, D. Van Hoomissen, Ozone 2022 Assesment. Annex: Summary of Abundances, Lifetimes, ODPs, REs, GWPs, GTPs., 2022.

[65] C.V. Vo, A.N. Paquet, An evaluation of the thermal conductivity of extruded polystyrene foam blown with HFC-134a or HCFC-142b, J. Cell. Plast. 40 (2004) 205–228, https://doi.org/10.1177/0021955×04043719.

[66] United Nations Environment Programme (UNEP), Montreal Protocol on Substances that Deplete the Ozone Layer., 1987. https://doi.org/10.18356/df488915-en-fr.

[67] C.V. Vo, R.T. Fox, Assessment of hydrofluoropropenes as insulating blowing agents for extruded polystyrene foams, J. Cell. Plast. 49 (2013) 423–438, https://doi.org/10.1177/0021955×13488398.

[68] Honeywell, SOLSTICE ® GAS BLOWING AGENT: A Low Global Warming Gas Blowing Agent to Improve Thermal Conductivity in XPS Production, 2023.

[69] Honeywell, HFO-1234ze(E): Properties and Application to Extruded Polystyrene, n.d.

[70] J.S. Colton, N.P. Suh, Nucleation of microcellular foam: theory and practice, Polym. Eng. Sci. 27 (1987) 500–503, https://doi.org/10.1002/pen.760270704.

[71] J.S. Colton, N.P. Suh, The nucleation of microcellular thermoplastic foam with additives: part II: experimental results and discussion, Polym. Eng. Sci. 27 (1987) 493–499, https://doi.org/10.1002/pen.760270703.

[72] S.K. Goel, E.J. Beckman, Generation of microcellular polymeric foams using supercritical carbon dioxide. I: effect of pressure and temperature on nucleation, Polym. Eng. Sci. 34 (1994) 1137–1147, https://doi.org/10.1002/pen.760341407.

[73] R. Gendron, M. Huneault, J. TatibouËt, C. Vachon, Foam extrusion of polystyrene blown with HFC-134a, Cell. Polym. 21 (2002) 315–342, https://doi.org/10.1177/026248930202100501.

[74] C. Vachon, R. Gendron, Foaming polystyrene with mixtures of carbon dioxide and HFC-134a, Cell. Polym. 22 (2003) 75–87, https://doi.org/10.1177/026248930302200201.

[75] I.C. Sanchez, R.H. Lacombe, An elementary molecular theory of classical fluids. Pure fluids, J. Phys. Chem. 80 (1976) 2352–2362, https://doi.org/10.1021/j100562a008.

[76] I.C. Sanchez, R.H. Lacombe, An elementary equation of state for polymer liquids, J. Polym. Sci. Polym. Lett. Ed. 15 (1977) 71–75, https://doi.org/10.1002/pol.1977.130150202.

[77] K. Von Konigslow, C.B. Park, R.B. Thompson, Polymeric foaming predictions from the sanchez-lacombe equation of state: application to polypropylene-carbon dioxide mixtures, Phys. Rev. Appl. 8 (2017) 1–14, https://doi.org/10.1103/PhysRevApplied.8.044009.

[78] Y. Sato, K. Fujiwara, T. Takikawa, Sumarno, S. Takishima, H. Masuoka, Solubilities and diffusion coefficients of carbon dioxide and nitrogen in polypropylene, high-density polyethylene, and polystyrene under high pressures and temperatures, Fluid Phase Equilib. 162 (1999) 261–276, https://doi.org/10.1016/S0378-3812(99)00217-4.

[79] R. Gendron, M.F. Champagne, Y. Delaviz, M.E. Polasky, Foaming polystyrene with a mixture of CO_2 and ethanol, J. Cell. Plast. 42 (2006) 127–138, https://doi.org/10.1177/0021955×06060948.

[80] S. Yeh, J. Yang, N. Chiou, T. Daniel, L.J. Lee, Introducing water as a coblowing agent in the carbon dioxide extrusion foaming process for polystyrene thermal insulation foams, Polym. Eng. Sci. 50 (2010) 1577–1584, https://doi.org/10.1002/pen.21624.

[81] C. Zhang, B. Zhu, D. Li, L.J. Lee, Extruded polystyrene foams with bimodal cell morphology, Polymers 53 (2012) 2435–2442, https://doi.org/10.1016/j.polymer.2012.04.006.

[82] K.M. Lee, E.K. Lee, S.G. Kim, C.B. Park, H.E. Naguib, Bi-cellular foam structure of polystyrene from extrusion foaming process, J. Cell. Plast. 45 (2009) 539–553, https://doi.org/10.1177/0021955×09343632.

[83] A. Raje, P. Georgopanos, J. Koll, J. LillepÄrg, U.A. Handge, V. Abetz, Open-celled foams from polyethersulfone/poly(ethylene glycol) blends using foam extrusion, Polym. (Basel) 15 (2023) 1–24, https://doi.org/10.3390/polym15010118.

[84] C.D. Han, Y.W. Kim, K.D. Malhotra, A study of foam extrusion using a chemical blowing agent, J. Appl. Polym. Sci. 20 (1976) 1583–1595, https://doi.org/10.1002/app.1976.070200615.

[85] Y. Oyanagi, J.L. White, Basic study of extrusion of polyethylene and polystyrene foams, J. Appl. Polym. Sci. 23 (1979) 1013–1026, https://doi.org/10.1002/app.1979.070230406.

[86] C.B. Park, D.F. Baldwin, N.P. Suh, Effect of the pressure drop rate on cell nucleation in continuous processing of microcellular polymers, Polym. Eng. Sci. 35 (1995) 432–440, https://doi.org/10.1002/pen.760350509.

[87] C.B. Park, A.H. Behravesh, R.D. Venter, Low density microcellular foam processing in extrusion using CO_2, Polym. Eng. Sci. 38 (1998) 1812–1823, https://doi.org/10.1002/pen.10351.

[88] X. Han, K.W. Koelling, D.L. Tomasko, L.J. Lee, Continuous microcellular polystyrene foam extrusion with supercritical CO_2, Polym. Eng. Sci. 42 (2002) 2094–2106, https://doi.org/10.1002/pen.11100.

[89] X.F. Peng, L.Y. Liu, B.Y. Chen, H.Y. Mi, X. Jing, A novel online visualization system for observing polymer extrusion foaming, Polym. Test. 52 (2016) 225–233, https://doi.org/10.1016/j.polymertesting.2016.04.023.

[90] S. Costeux, D. Foether, Continuous extrusion of nanocellular foam, Annu. Tech. Conf. - ANTEC Conf. Proc. (2015) 2740–2745.

[91] V. Bernardo, J. Martin-de Leon, M.A. Rodriguez-Perez, Anisotropy in nanocellular polymers promoted by the addition of needle-like sepiolites, Polym. Int. 68 (2019) 1204–1214, https://doi.org/10.1002/pi.5813.

[92] J. Pinto, M. Dumon, M. Pedros, J. Reglero, M.A. Rodriguez-Perez, Nanocellular CO_2 foaming of PMMA assisted by block copolymer nanostructuration, Chem. Eng. J. 243 (2014) 428–435, https://doi.org/10.1016/j.cej.2014.01.021.

[93] J. Pinto, M. Dumon, M.A. Rodriguez-Perez, R. Garcia, C. Dietz, Block copolymers self-assembly allows obtaining tunable micro or nanoporous membranes or depth filters based on PMMA; Fabrication method and nanostructures, J. Phys. Chem. C. 118 (2014) 4656–4663, https://doi.org/10.1021/jp409803u.

[94] M. Merillas, M.Á. RodrÍguez-PÉrez, J.L. Pura, J. MartÍn-de LeÓn, V. Bernardo, SAS copolymer induced nucleation in PS-based open-cell nanocellular polymers, Mater. Today Chem. 48 (2025), https://doi.org/10.1016/j.mtchem.2025.102905.

[95] C. Okolieocha, T. KÖppl, S. Kerling, F.J. TÖlle, A. Fathi, R. MÜlhaupt, V. AltstÄdt, Influence of graphene on the cell morphology and mechanical properties of extruded polystyrene foam, J. Cell. Plast. 51 (2015) 413–426, https://doi.org/10.1177/0021955×14566084.

[96] H.E. Naguib, C.B. Park, P.C. Lee, Effect of talc content on the volume expansion ratio of extruded PP foams, J. Cell. Plast. 39 (2003) 499–511, https://doi.org/10.1177/002195503039247.

[97] B.V. Kichatov, A.M. Korshunov, Nucleation of gas bubbles in extrusion foaming of high-pressure polyethylene, Theor. Found. Chem. Eng. 39 (2005) 643–652, https://doi.org/10.1007/s11236-005-0129-x.

[98] S. Pilla, S.G. Kim, G.K. Auer, S. Gong, C.B. Park, Microcellular extrusion foaming of poly(lactide)/poly(butylene adipate-co-terephthalate) blends, Mater. Sci. Eng. C. 30 (2010) 255–262, https://doi.org/10.1016/j.msec.2009.10.010.

[99] M. Nofar, Effects of nano-/micro-sized additives and the corresponding induced crystallinity on the extrusion foaming behavior of PLA using supercritical CO_2, Mater. Des. 101 (2016) 24–34, https://doi.org/10.1016/j.matdes.2016.03.147.

[100] X. Han, C. Zeng, L.J. Lee, K.W. Koelling, D.L. Tomasko, Extrusion of polystyrene nanocomposite foams with supercritical CO 2, Polym. Eng. Sci. 43 (2003) 1261–1275, https://doi.org/10.1002/pen.10107.

[101] C. Zhang, B. Zhu, L.J. Lee, Extrusion foaming of polystyrene/carbon particles using carbon dioxide and water as co-blowing agents, Polym. (Guildf.) 52 (2011) 1847–1855, https://doi.org/10.1016/j.polymer.2011.02.016.

[102] M. Keshtkar, M. Nofar, C.B. Park, P.J. Carreau, Extruded PLA/clay nanocomposite foams blown with supercritical CO_2, Polym. (Guildf.) 55 (2014) 4077–4090, https://doi.org/10.1016/j.polymer.2014.06.059.

[103] W. Zhai, T. Kuboki, L. Wang, C.B. Park, E.K. Lee, H.E. Naguib, Cell structure evolution and the crystallization behavior of polypropylene/clay nanocomposites foams blown in continuous extrusion, Ind. Eng. Chem. Res. 49 (2010) 9834–9845, https://doi.org/10.1021/ie101225f.

[104] F. Zandi, M. Rezaei, A. Kasiri, Effect of nanoclay on the physical-mechanical and thermal properties and microstructure of extruded noncross-linked LDPE nanocomposite foams, Key Eng. Mater. 471–472 (2011) 751–756, https://doi.org/10.4028/www.scientific.net/KEM.471-472.751.

[105] L.M. Matuana, C. a Diaz, Study of cell nucleation in microcellular poly(lactic acid) foamed with supercritical CO_2 through a continuous-extrusion process, Ind. Eng. Chem. Res. 49 (2010) 2186–2193, https://doi.org/10.1021/ie9011694.

[106] Y. Fei, W. Fang, M. Zhong, J. Jin, P. Fan, J. Yang, Z. Fei, L. Xu, F. Chen, Extrusion foaming of lightweight polystyrene composite foams with controllable cellular structure for sound absorption application, Polym. (Basel) 11 (2019), https://doi.org/10.3390/polym11010106.

[107] J. Shen, X. Han, L.J. Lee, Nanoscaled reinforcement of polystyrene foams using carbon nanofibers, J. Cell. Plast. 42 (2006) 105–126, https://doi.org/10.1177/0021955×06060947.

[108] M. Fasihi, A.A. Targhi, H. Bayat, The simultaneous effect of nucleating and blowing agents on the cellular structure of polypropylene foamed via the extrusion process, E-Polym. 16 (2016) 235–241, https://doi.org/10.1515/epoly-2016-0033.

[109] P. Yu, G. Liu, K. Li, A. Huang, B. Chen, H. Mi, S. Zhang, X. Peng, Fabrication of polystyrene/nano-CaCO3 foams with unimodal or bimodal cell structure from extrusion foaming using supercritical carbon dioxide, Polym. Compos 37 (2016) 1864–1873, https://doi.org/10.1002/pc.23361.

[110] M. Aksit, B. Klose, C. Zhao, K. Kreger, H.W. Schmidt, V. AltstÄdt, Morphology control of extruded polystyrene foams with benzene-trisamide-based nucleating agents, J. Cell. Plast. 55 (2019) 249–261, https://doi.org/10.1177/0021955×19837508.

[111] A. Rizvi, A. Tabatabaei, M.R. Barzegari, S.H. Mahmood, C.B. Park, situ fibrillation of CO_2-philic polymers: sustainable route to polymer foams in a continuous process, Polym. (Guildf.) 54 (2013) 4645–4652, https://doi.org/10.1016/j.polymer.2013.06.023.

[112] K. Wang, F. Wu, W. Zhai, W. Zheng, Effect of polytetrafluoroethylene on the foaming behaviors of linear polypropylene in continuous extrusion, J. Appl. Polym. Sci. 129 (2013) 2253–2260, https://doi.org/10.1002/app.38959.

[113] W. Zhai, J. Yu, L. Wu, W. Ma, J. He, Heterogeneous nucleation uniformizing cell size distribution in microcellular nanocomposites foams, Polym. (Guildf.) 47 (2006) 7580–7589, https://doi.org/10.1016/j.polymer.2006.08.034.

[114] C. Forest, P. Chaumont, P. Cassagnau, B. Swoboda, P. Sonntag, CO_2 nano-foaming of nanostructured PMMA, Polym. (Guildf.) 58 (2015) 76–87, https://doi.org/10.1016/j.polymer.2014.12.048.
[115] A. Huang, P. Yu, X. Jing, H.Y. Mi, L.H. Geng, B.Y. Chen, X.F. Peng, The effect of talc on the mechanical, crystallization and foaming properties of poly(lactic acid), J. Macromol. Sci. Part B Phys. 55 (2016) 908–924, https://doi.org/10.1080/00222348.2016.1217186.
[116] J. Pan, D. Zhang, M. Wu, S. Ruan, J.M. Castro, L.J. Lee, F. Chen, Impacts of carbonaceous particulates on extrudate semicrystalline polyethylene terephthalate foams: nonisothermal crystallization, rheology, and infrared attenuation studies, Ind. Eng. Chem. Res. 59 (2020) 15586–15597, https://doi.org/10.1021/acs.iecr.0c02929.
[117] X. Han, C. Zeng, L.J. Lee, K.W. Koelling, D.L. Tomasko, Extrusion of polystyrene nanocomposite foams with supercritical CO 2, Polym. Eng. Sci. 43 (2003) 1261–1275, https://doi.org/10.1002/pen.10107.
[118] S.H. Lee, Y. Zhang, M. Kontopoulou, C.B. Park, A. Wong, W. Zhai, Optimization of dispersion of nanosilica particles in a PP matrix and their effect on foaming, Int. Polym. Process 26 (2011) 388–398, https://doi.org/10.3139/217.2403.
[119] M. Aksit, C. Zhao, B. Klose, K. Kreger, H.W. Schmidt, V. AltstÄdt, Extruded polystyrene foams with enhanced insulation and mechanical properties by a benzene-trisamide-based additive, Polym. (Basel) 11 (2019) 1–10, https://doi.org/10.3390/polym11020268.
[120] C.B. Park, L.K. Cheung, Seung-Won Song, The effect of talc on cell nucleation in extrusion foam processing of polypropylene with CO_2 and isopentane, Cell. Polym. 17 (1998) 221–251, https://doi.org/10.1177/026248931981704001.
[121] H.E. Naguib, C.B. Park, N. Reichelt, Fundamental foaming mechanisms governing the volume expansion of extruded polypropylene foams, J. Appl. Polym. Sci. 91 (2004) 2661–2668, https://doi.org/10.1002/app.13448.
[122] H.E. Naguib, C.B. Park, P.C. Lee, D. Xu, A study on the foaming behaviors of PP resins with talc as nucleating agent, J. Polym. Eng. 26 (2006) 565–587, https://doi.org/10.1515/POLYENG.2006.26.6.565.
[123] J. Wang, P.C. Lee, C.B. Park, Visualization of initial expansion behavior of butane-blown low-density polyethylene foam at extrusion die exit, Polym. Eng. Sci. 51 (2011) 492–499, https://doi.org/10.1002/pen.21803.
[124] V. Mittal, Polymer layered silicate nanocomposites: a review, Materials 2 (2009) 992–1057, https://doi.org/10.3390/ma2030992.
[125] F. Guo, S. Aryana, Y. Han, Y. Jiao, A review of the synthesis and applications of polymer-nanoclay composites, Appl. Sci. 8 (2018) 1–29, https://doi.org/10.3390/app8091696.
[126] P. Saraeian, H.R. Tavakoli, A. Ghassemi, Production of polystyrene-nanoclay nanocomposite foam and effect of nanoclay particles on foam cell size, J. Compos. Mater. 47 (2013) 2211–2217, https://doi.org/10.1177/0021998312454906.
[127] X. Lian, W. Mou, T. Kuang, X. Liu, S. Zhang, F. Li, T. Liu, X. Peng, Synergetic effect of nanoclay and nano-CaCO3 hybrid filler systems on the foaming properties and cellular structure of polystyrene nanocomposite foams using supercritical CO_2, Cell. Polym. 39 (2020) 185–202, https://doi.org/10.1177/0262489319900948.
[128] A. Ballesteros, E. Laguna-Gutierrez, P. Cimavilla-Roman, M.L. Puertas, A. Esteban-Cubillo, J. Santaren, M.A. Rodriguez-Perez, Influence of the dispersion of Nanoclays on the cellular structure of foams based on polystyrene, J. Appl. Polym. Sci. 138 (2021), https://doi.org/10.1002/app.51373.
[129] K. Wang, Y. Pang, F. Wu, W. Zhai, W. Zheng, Cell nucleation in dominating formation of bimodal cell structure in polypropylene/polystyrene blend foams prepared via continuous extrusion with supercritical CO_2, J. Supercrit. Fluids 110 (2016) 65–74, https://doi.org/10.1016/j.supflu.2015.12.012.
[130] A. Cunningham, D.J. Sparrow, Rigid polyurethane foam: what makes it the most effective insulant? Cell. Polym. 5 (1986) 327–342, https://doi.org/10.1177/026248938600500501.
[131] C.V. Vo, F. Bunge, J. Duffy, L. Hood, Advances in thermal insulation of extruded polystyrene foams, Cell. Polym. 30 (2011) 137–156, https://doi.org/10.1177/026248931103000303.
[132] J. Shen, C. Zeng, L.J. Lee, Synthesis of polystyrene-carbon nanofibers nanocomposite foams, Polymers 46 (2005) 5218–5224, https://doi.org/10.1016/j.polymer.2005.04.010.
[133] C. Zeng, N. Hossieny, C. Zhang, B. Wang, Synthesis and processing of PMMA carbon nanotube nanocomposite foams, Polym. (Guildf.) 51 (2010) 655–664, https://doi.org/10.1016/j.polymer.2009.12.032.
[134] P. Gong, M.P. Tran, P. Buahom, C. Detrembleur, J.M. Thomassin, S. Kenig, Q. Wang, C.B. Park, Thermal insulation foam of polystyrene/expanded graphite composite with reduced radiation and conduction, Polymers 17 (2025), https://doi.org/10.3390/polym17081040.
[135] Q.B. Ho, M. Kontopoulou, Stabilization of the cellular structure of polypropylene foams and secondary nucleation mechanism in the presence of graphene nanoplatelets, Polymers 198 (2020) 122506, https://doi.org/10.1016/j.polymer.2020.122506.
[136] C. Wang, S. Ying, Z. Xiao, Preparation of short carbon fiber/polypropylene fine-celled foams in supercritical CO_2, J. Cell. Plast. 49 (2013) 65–82, https://doi.org/10.1177/0021955×12459642.
[137] S. Jin, J. Yang, C. Pu, L. Yang, Y. Zhou, Application of graphene oxide with variable spatial structure as a key to polyethylene foaming through cured CO_2 as foaming agent, J. Inorg. Organomet. Polym. Mater. (2025), https://doi.org/10.1007/s10904-025-03615-9.
[138] J. MartÍn-de LeÓn, A. Sillero, M.A. RodrÍguez-PÉrez, Using infrared opacifiers to reduce the thermal conductivity of micro and nanocellular polymethylmethacrylate, Polym. (Guildf.) 290 (2024), https://doi.org/10.1016/j.polymer.2023.126523.
[139] S. Yeh, C. Huang, C. Su, K. Cheng, T. Chuang, W. Guo, S. Wang, Effect of dispersion method and process variables on the properties of supercritical CO 2 foamed polystyrene/graphite nanocomposite foam, Polym. Eng. Sci. 53 (2013) 2061–2072, https://doi.org/10.1002/pen.23468.
[140] M. Arduini, J. Manara, C. Vo, Modeling of radiative properties of polystyrene foams containing IR-opacifiers, Cell. Polym. 35 (2016) 49–66, https://doi.org/10.1177/026248931603500201.
[141] I. SÁnchez-CalderÓn, F. Lizalde-Arroyo, J. MartÍn-de-LeÓn, M.Á. RodrÍguez-PÉrez, V. Bernardo, Improvement of the thermal conductivity of micronized nanocellular poly(methyl-methacrylate) (PMMA) by adding infrared blockers, Constr. Build. Mater. 470 (2025) 18–20, https://doi.org/10.1016/j.conbuildmat.2025.140522.
[142] J. Ding, W. Ma, F. Song, Q. Zhong, Effect of nano-Calcium Carbonate on microcellular foaming of polypropylene, J. Mater. Sci. 48 (2013) 2504–2511, https://doi.org/10.1007/s10853-012-7039-1.
[143] F.C. Chiu, S.M. Lai, C.M. Wong, C.H. Chang, Properties of calcium carbonate filled and unfilled polystyrene foams prepared using supercritical carbon dioxide, J. Appl. Polym. Sci. 102 (2006) 2276–2284, https://doi.org/10.1002/app.24424.
[144] A.H. Behravesh, C.B. Park, L.K. Cheung, R.D. Venter, Extrusion of polypropylene foams with hydrocerol and isopentane, J. Vinyl Addit. Technol. 2 (1996) 349–357, https://doi.org/10.1002/vnl.10153.
[145] T. Garbacz, A. Tor-Świątek, V. SedlaŘÍk, Characterization of mechanical and thermal properties of PLA/blowing agents composites, AIP Conf. Proc. 2205 (2020) 1–6, https://doi.org/10.1063/1.5142949.
[146] F.A. Soares, S.M.B. Nachtigall, Effect of chemical and physical foaming additives on the properties of PP/wood flour composites, Polym. Test. 32 (2013) 640–646, https://doi.org/10.1016/j.polymertesting.2013.02.009.
[147] D. Kropp, W. Michaeli, T. Herrmann, O. SchrÖder, Foam extrusion of thermoplastic elastomers using CO_2 as blowing agent, J. Cell. Plast. 34 (1998) 304–311, https://doi.org/10.1177/0021955×9803400402.
[148] M. Stumpf, A. SpÖrrer, H.W. Schmidt, V. AltstÄdt, Influence of supramolecular additives on foam morphology of injection-molded i-PP, J. Cell. Plast. 47 (2011) 519–534, https://doi.org/10.1177/0021955×11408769.
[149] M. MÖrl, C. Steinlein, K. Kreger, H.W. Schmidt, V. AltstÄdt, Improved compression properties of polypropylene extrusion foams by supramolecular additives, J. Cell. Plast. 54 (2018) 483–498, https://doi.org/10.1177/0021955×17695096.
[150] S. Wang, P. Xue, M. Jia, J. Tian, R. Zhang, Effect of polymer blends on the properties of foamed wood-polymer composites, Mater. (Basel) 12 (2019) 1971, https://doi.org/10.3390/ma12121971.
[151] P.C. Lee, J. Wang, C.B. Park, Extrusion of microcellular open-cell LDPE-based sheet foams, J. Appl. Polym. Sci. 102 (2006) 3376–3384, https://doi.org/10.1002/app.24868.
[152] Y. Pang, S. Wang, M. Wu, W. Liu, F. Wu, P.C. Lee, W. Zheng, Kinetics study of oil sorption with open-cell polypropylene/polyolefin elastomer blend foams prepared via continuous extrusion foaming, Polym. Adv. Technol. 29 (2018) 1313–1321, https://doi.org/10.1002/pat.4243.
[153] S.G. Mosanenzadeh, H.E. Naguib, C.B. Park, N. Atalla, Development of polylactide open-cell foams with bimodal structure for high-acoustic absorption, J. Appl. Polym. Sci. 131 (2014) 1–11, https://doi.org/10.1002/app.39518.
[154] J. Ju, J. Zhao, C. Li, Y. Xue, Vacuum insulation panel production with ultralow thermal conductivity—a review, Int. J. Thermophys. 45 (2024) 1–21, https://doi.org/10.1007/s10765-024-03461-w.
[155] E. Laguna-Gutierrez, R. Van Hooghten, P. Moldenaers, M.A. Rodriguez-Perez, Understanding the foamability and mechanical properties of foamed polypropylene blends by using extensional rheology, J. Appl. Polym. Sci. 132 (2015) 1–14, https://doi.org/10.1002/app.42430.
[156] M. Mihai, M.A. Huneault, B.D. Favis, Rheology and extrusion foaming of chain-branched poly(lactic acid), Polym. Eng. Sci. 50 (2010) 629–642, https://doi.org/10.1002/pen.21561.
[157] J. Ludwiczak, M. Kozlowski, Foaming of polylactide in the presence of chain extender, J. Polym. Environ. 23 (2015) 137–142, https://doi.org/10.1007/s10924-014-0658-7.
[158] K. Bocz, B. MolnÁr, G. Marosi, F. Ronkay, Preparation of low-density microcellular foams from recycled PET modified by solid state polymerization and chain extension, J. Polym. Environ. 27 (2019) 343–351, https://doi.org/10.1007/s10924-018-1351-z.
[159] L. Di Maio, I. Coccorullo, S. Montesano, L. Incarnato, Chain extension and foaming of recycled PET in extrusion equipment, Macromol. Symp. 228 (2005) 185–200, https://doi.org/10.1002/masy.200551017.
[160] S. Pilla, S.G. Kim, G.K. Auer, S. Gong, C.B. Park, Microcellular extrusion-foaming of polylactide with chain-extender, Polym. Eng. Sci. 49 (2009) 1653–1660, https://doi.org/10.1002/pen.21385.
[161] P.C. Lee, G. Li, J.W.S. Lee, C.B. Park, Improvement of cell opening by maintaining a high temperature difference in the surface and core of a foam extrudate, J. Cell. Plast. 43 (2007) 431–444, https://doi.org/10.1177/0021955×07079150.
[162] P.C. Lee, H.E. Naguib, C.B. Park, J. Wang, Increase of open-cell content by plasticizing soft regions with secondary blowing agent, Polym. Eng. Sci. 45 (2005) 1445–1451, https://doi.org/10.1002/pen.20422.
[163] P.C. Lee, J. Wang, C.B. Park, Extruded open-cell foams using two semicrystalline polymers with different crystallization temperatures, Ind. Eng. Chem. Res. 45 (2006) 175–181, https://doi.org/10.1021/ie050498j.
[164] A. Rizvi, R.K.M. Chu, J.H. Lee, C.B. Park, Superhydrophobic and oleophilic open-cell foams from fibrillar blends of polypropylene and polytetrafluoroethylene, ACS Appl. Mater. Interfaces 6 (2014) 21131–21140, https://doi.org/10.1021/am506006v.

[165] S. Wang, K. Wang, Y. Pang, Y. Li, F. Wu, S. Wang, W. Zheng, Open-cell polypropylene/polyolefin elastomer blend foams fabricated for reusable oil-sorption materials, J. Appl. Polym. Sci. 133 (2016) 1–10, https://doi.org/10.1002/app.43812.
[166] B. Li, G. Zhao, G. Wang, L. Zhang, J. Gong, Z. Shi, Biodegradable PLA/PBS open-cell foam fabricated by supercritical CO_2 foaming for selective oil-adsorption, Sep. Purif. Technol. 257 (2021), https://doi.org/10.1016/j.seppur.2020.117949.
[167] M. Mihai, M.A. Huneault, B.D. Favis, H. Li, Extrusion foaming of semi-crystalline PLA and PLA/thermoplastic starch blends, Macromol. Biosci. 7 (2007) 907–920, https://doi.org/10.1002/mabi.200700080.
[168] M. Chauvet, M. Sauceau, F. Baillon, J. Fages, Mastering the structure of PLA foams made with extrusion assisted by supercritical CO_2, J. Appl. Polym. Sci. 134 (2017) 1–10, https://doi.org/10.1002/app.45067.
[169] K.A. Shah, R.Q. Albuquerque, C. BrÜtting, H. RuckdÄschel, Machine learning-based time series analysis of polylactic acid bead foam extrusion, J. Appl. Polym. Sci. 141 (2024) 1–11, https://doi.org/10.1002/app.56170.
[170] A. Xiang, D. Yin, Y. He, Y. Li, H. Tian, Multifunctional nucleating agents with simultaneous plasticizing, solubilizing, nucleating and their effect on polyvinyl alcohol foams, J. Supercrit. Fluids 170 (2021) 105156, https://doi.org/10.1016/j.supflu.2020.105156.
[171] T. Ono, S. Yoda, D. Kageyama, Y. Saito, Y. Takebayashi, T. Tai, M. Otani, Computational design of nucleating agents of poly (methyl methacrylate) microcellular foams: "savanna-like" surface structures and their effects on foaming, Polym. Eng. Sci. 63 (2023) 4019–4031, https://doi.org/10.1002/pen.26502.
[172] X. Liu, S. Jin, Z. Shi, H. Cong, W. Gong, Y. Zhou, Polypropylene synergistically nucleated by a novel β-nucleating and foaming nucleating agent: foaming performance and material properties (English Ed), Iran. Polym. J. 33 (2024) 355–366, https://doi.org/10.1007/s13726-023-01254-w.